`

Chapter One

Introduction

1.1 Introduction

Breast cancer is the most frequent cancer among women, impacting 2.1 million women each year, and also causes the greatest number of cancer-related deaths among women. In 2018, it is estimated that 627,000 women died from breast cancer – that is approximately 15% of all cancer deaths among women. While breast cancer rates are higher among women in more developed regions, rates are increasing in nearly every region globally.(WHO 2018).

The first noticeable symptom of breast cancer is typically a lump that feels different from the rest of the breast tissue. More than 80% of breast cancer cases are discovered when the woman feels a lump. Lumps found in lymph nodes located in the armpits can also indicate breast cancer (Merck *2003)*.

Indications of breast cancer other than a lump may include thickening different from the other breast tissue, one breast becoming larger or lower, a nipple changing position or shape or becoming inverted, skin puckering or dimpling, a rash on or around a nipple, discharge from nipple/s, constant pain in part of the breast or armpit, and swelling beneath the armpit or around the collarbone (Watson M (2008). Pain ("mastodynia") is an unreliable tool in determining the presence or absence of breast cancer, but may be indicative of other breast health issues (eMedicine 2006).

Inflammatory breast cancer is a particular type of breast cancer which can pose a substantial diagnostic challenge. Symptoms may resemble a breast inflammation and may include itching, pain, swelling, nipple inversion, warmth and redness

`

throughout the breast, as well as an orange-peel texture to the skin referred to aspeau d'orange; as inflammatory breast cancer doesn't show as a lump there's sometimes a delay in diagnosis (Merck *2003)*.

Another reported symptom complex of breast cancer is Paget's disease of the breast. This syndrome presents as skin changes resembling eczema, such as redness, discoloration, or mild flaking of the nipple skin. As Paget's disease of the breast advances, symptoms may include tingling, itching, increased sensitivity, burning, and pain. There may also be discharge from the nipple. Approximately half of women diagnosed with Paget's disease of the breast also have a lump in the breast (NCI 2005).

In rare cases, what initially appears as a fibroadenoma (hard, movable non-cancerous lump) could in fact be a phyllodes tumor. Phyllodes tumors are formed within the stroma (connective tissue) of the breast and contain glandular as well as stromal tissue. Phyllodes tumors are not staged in the usual sense; they are classified on the basis of their appearance under the microscope as benign, borderline, or malignant (answers.com).

Occasionally, breast cancer presents as metastatic disease—that is, cancer that has spread beyond the original organ. The symptoms caused by metastatic breast cancer will depend on the location of metastasis. Common sites of metastasis include bone, liver, lung and brain (*Lacroix 2006*). Unexplained weight loss can occasionally signal breast cancer, as can symptoms of fevers or chills. Bone or joint pains can sometimes be manifestations of metastatic breast cancer, as can jaundice or neurological symptoms. These symptoms are called non-specific, meaning they could be manifestations of many other illnesses (NCI 2004).

Most symptoms of breast disorders, including most lumps, do not turn out to represent underlying breast cancer. Fewer than 20% of lumps, for example, are

`

cancerous (NCI 2004), and benign breast diseases such as mastitis and fibro adenoma of the breast are more common causes of breast disorder symptoms. Nevertheless, the appearance of a new symptom should be taken seriously by both patients and their doctors, because of the possibility of an underlying breast cancer at almost any age (Merck *2003).*

Mammography (also called mastography) is the process of using low-energy X-rays (usually around 30 kVp) to examine the human breast for diagnosis and screening. The goal of mammography is the early detection of breast cancer, typically through detection of characteristic masses or microcalcifications.

As with all X-rays, mammograms use doses of ionizing radiation to create images. These images are then analyzed for abnormal findings. It is usual to employ lower-energy X-rays, typically Mo (K-shell x-ray energies of 17.5 and 19.6 keV) and Rh (20.2 and 22.7 keV) than those used for radiography of bones. Ultrasound, ductography, positron emission mammography (PEM), and magnetic resonance imaging (MRI) are adjuncts to mammography. Ultrasound is typically used for further evaluation of masses found on mammography or palpable masses not seen on mammograms. Ductograms are still used in some institutions for evaluation of bloody nipple discharge when the mammogram is non-diagnostic. MRI can be useful for further evaluation of questionable findings, as well as for screening pre-surgical evaluation in patients with known breast cancer, in order to detect additional lesions that might change the surgical approach, for example, from breast-conserving lumpectomy to mastectomy. Other procedures being investigated include tomosynthesis (Basset and Kimme, 1991).

Texture analysis refers to the branch of imaging that is concerned with the description of characteristic of image properities by textural feature, in general different researches used different definition depending upon the particular area of

`

application, so the texture analysis is defined as the spatial variation of pixel intensities so the main image processing discipline in which texture analysis technique is used are: classification, segmentation and synthesis. Texture analysis describes a variety of image-analysis techniques that quantify the variation in surface intensity or patterns, including some that are imperceptible to the human visual system. Texture analysis may be particularly well-suited for lesion segmentation and characterization and for the longitudinal monitoring of disease or recovery. Texture analysis is tremendously versatile and can be applied to virtually any digital image. If the spatial extent of the lesion can be identified by an independent means, then the application of texture analysis can be restricted to a set of predefined regions of interest (e.g. lesion versus “normal” or contra-lateral reference). In the selection of image region of interest or image size, the investigator or analyst will have to balance the need to capture sufficient textural information for classification purposes with the desire to avoid including objects that span multiple tissue categories (tuceryan , 1998).

1.1.Problem of study:

The understanding of the cognitive process of human vision is constantly expanding much has been learn from the experiment of the visual perception of the image information (Bruce et. al, 2003) although the use of mammographic images in detection, diagnosis and mass margin identification throughout the breast quadrant still not the border line for diagnosis. The main issue is the detection of the scattered microscopic tumor cell around its mass; therefore the use of texture analysis technique will make CTV definition and outlining it very accurately to be used in treatment criteria for this type of mass.

`

1.2. Objectives of the Study:

1.2.1. General Objective:

The general objective of this study is to characterize the breast masses in X-ray mammographic images by using image texture analysis in order to recognize the tumor and its surroundings by its texture feature.

1.2.2. Specific Objectives:

- To write an algorithm and function that can be used to extract feature from mammogram images.
- To extract feature from breast tissue (fat, gland and connective) and breast mass (ROI).
- To classify the extracted feature using first order statistic.
- To classify the extracted feature using higher order statistics.
- To classify the extracted feature using linear discriminate analysis.

1.3. Significant of study:

This study will highlight on evaluation of tumor extra marginal detection using image processing programs (IDL), once we need faster and accurate diagnostic modalities in this situation in order to have high diagnostic accuracy in assessing breast tumors and therefore using this scans to plan patient for treatment which need Avery accurate delineation of tumor edges in case of CTV and planning target volume in order to deliver sufficient dose in case of radiation to the both volumes and increase therapeutic and diagnostic radio.

`

1.4. Overview of the study:

This study consists of five chapters, with chapter one is an introduction introduce briefly this thesis and will contain (overview of breast cancer, mammography and texture analysis) problem of study also contain general, specific objectives, significant of study and the overview of the study). Chapter two is literature review about breast anatomy, physiology and pathology, mammography and texture analysis. Chapter three will describe the methodology (material, method) will be use. Chapter four will include presentation (result) of final of study; chapter five is discussion, conclusion and recommendation for future scope in addition to references and appendices.

`

Chapter Two

Theoretical Background

2.1. Anatomy and physiology of the breast:

The breasts are specialized accessory glands of the skin that secrete milk (Fig. 2-1). They are present in both sexes. In males and immature females, they are similar in structure. The nipples are small and surrounded by a colored area of skin called the areola (Snell, 8th edition).

The breast consists of gland tissue, fibrous tissue, connecting its lobes and fatty tissue in the intervals between lobes. The breast contains 15 to 20 lobes of glandular tissue, which constitute the parenchyma of the mammary gland. These lobes give a shape characteristic to the breast due to a considerable amount of fat, and these are composed of lobules, connected together by areolar tissue, blood vessels and ducts. Each lobule is drained by a lactiferous duct, which opens independently on the nipple. Just deep to the areola, each duct has a dilated portion, the lactiferous sinus, which accumulates milk during lactation. The smallest lobules include also the alveoli, which open into the smallest branches of the lactiferous ducts (Dixon, 2006).

During the fetal period is created, by epidermis, a depression which forms a mammary pit on the local of mammary gland. The region where the mammary glands appear is located in left and right sides of the upper ventral region of the trunk. The breasts exist in woman and man, but the mammary glands are normally most developed in female, except in some particular circumstances related with hormonal problems. The nipple is a small conical prominence surrounded by a circular area of pigmented skin, the areola, which contains large sebaceous glands that are often invisible to the naked eye. The base of the female breast, roughly circular, extends from the second rib above to the sixth rib below. Medially, it

`

borders the lateral edge of the body of the sternum and laterally it reaches the mid auxiliary line in Figure 3 (Moinfar, 2007).

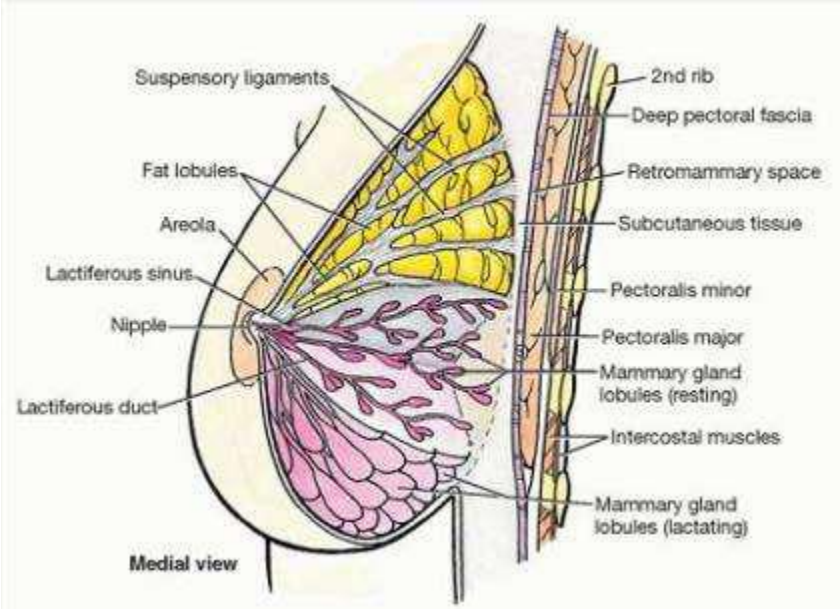

Figure 2.1. Anatomy of breast (Moinfar, 2007 and Moore et al, 2004).

At puberty, the female breasts normally grow according to the glandular development and increase of fat deposition; furthermore, also the nipples and areolas grow. The size and shape of breast depends on genetic, racial and dietary factors. During the pregnancy, the areola color becomes dark, and after that keeps the pigmentation. This color diminishes as soon as lactation is over, but is never entirely lost throughout life (Moore et al, 2004).

Children breast consists principally ducts with dispersed alveoli, being similar in adipose deposition and the growth of the mammary glands, as well as the initial development of lobules and alveoli of the breast. Progesterone and prolactin which cause the final growth, are responsible for the function of these structures and cause the external appearance of the mature female breast (Guyton and Hall,2000).

Cancer is a condition that affects people all over the world. Research in this area began in 1900 and cancer was considered a disease without cure. As other cancers,

`

breast cancer arises when cells grow and multiply uncontrollably, which produces a tumor or a neoplasm. The tumors can be benign when the cancerous cells do not invade other body tissues or malignant if cells attack nearby tissues and travel through the bloodstream or lymphatic system to other parts of the body, spreading a cancer by a process known as metastasis (Seeley, 2004).

2.2. Breast pathologies:

2.2.1. Fibroadenoma:

Fibroadenomas are the most common breast tumors in pubertal females, and there are three types of fibroadenoma classified as: common, giant and juvenile. These tumors are characterized by a proliferation of both glandular and stromal elements, have welldemarcated borders and are firm, rubbery, freely mobile, solid, usually solitary breast masses. There is no pain or tenderness due to fibroadenomas and their size do not change with the menstrual cycle. Women aged in their 20s and adolescents are the most common people affected with this disease. A rapid growth sometimes occurs but usually that growth is extremely slow. A giant fibroadenoma should measure over 5 cm in diameter but the average is 2.5 cm. These tumors may return (approximately 20% recur), women should be aware of this risk and have periodic examinations (Dixon, 2006).

2.2.2. Mammary Dysplasia:

Mammary dysplasia also can be called as fibrocystic changes (FCC), fibrocystic disease, fibrous mastopathy or fibroadenosis cystic. In reality, these alterations not indicate a disease. This pathology is the defined as being a benign alteration of the breast consisting of cystic dilatation of intralobular glands with or without stromal fibrosis. The age distribution of this lesion is between 20 and 50 years. Normally, fibrocystic changes are associated to the cyclic levels of ovarian hormones, because during ovulation and before menstruation, hormone level changes often

`

cause the breast cells to retain fluid and develop into nodules or cysts, which feel like a lump when touched. The texture of the breast is, in these cases, similar to the breast in pre-menstrual phase. The signs of fibrocystic changes include increased engorgement and density of the breasts, excessive nodularity, rapid change and fluctuation in the size of cystic areas, increased tenderness, and occasionally spontaneous nipple discharge. It can be unilateral, bilateral or just affect a part of the breast (Malik, 2010).

2.2.3. Mastitis and breast abscess :

Inflammatory conditions of the breast, particularly acute mastitis and breast abscess are rare pathologies. Often these infections can happen in postpartum situations or after a lesion. There are two types of mastitis: acute and chronic. In acute mastitis, it is predominantly composed of neutrophilic granulocytes, seen mostly in lactating women. Chronic mastitis may be due to reinfection or a relapsed infection; the first case occurs sporadically and commonly is transmitted from the baby, and the second case means that eradication of the pathogen was failed.

Breast abscess arises when mastitis was treated inadequately and exist milk retention. The useful diagnosis techniques used to treat include ultrasonography of the breast and needle aspiration under local anesthesia with a purpose of identifies collections of fluid or pus (Jatoi, 2010).

2.2.4. Breast Cancer:

Cancer is a condition that affects people all over the world. Research in this area beginning since 1900 and cancer was o disease without cure. As other cancers, breast cancer arises when cells growth and multiply uncontrollably, which produces a tumor or a neoplasm. The tumors can be benign when the cancerous cells do not invade other body tissues or malignant if cells attack nearby tissues

`

and travel through the bloodstream or lymphatic system to other parts of the body, spreading a cancer by a process known as metastasis (Alvin, 2006; Panno, 2005). The damage that cancerous tumors cause to various important organs in the body can lead to serious illness, so an early detection is important for a better treatment and recovery. The most common range of age attacked by breast cancer is between 40-50 years old and until the menopause, the breast cancer rate incidence increase decreases dramatically. There are other risk factors that lead to develop a breast cancer as like age at menarche and menopause, age at first pregnancy, family history, previous benign breast disease and radiation (Dixon, 2006).

2.2.5. Types of Breast cancer:

Breast cancer can be classified into invasive/infiltrating or non-invasive/in situ, and both have characteristic patterns by which they can be classified. The noninvasive breast cancer is divided into ductal and lobular types and as the names induce ductal carcinomas arise from ducts and lobular carcinomas arise from lobules and do not destroy other tissues (Jatoi, 2010). Ductal carcinoma in situ (DCIS) is the most common form of noninvasive carcinoma. The most common mammographic manifestation of DCIS is microcalcifications, and usually it is more easily to diagnose microcalcifications than masses, and thus is more effortlessly to detect DCIS than infiltrating carcinoma. This carcinoma is characterized by the proliferation of malignant mammary ductal epithelial cells that line the breast milk ducts, without evidence of invasion beyond the basement membrane. Once is important the size and extent of a DCIS to determineoptimal surgical management and mammography had difficulties some studies demonstrate most interest in other modalities, such as magnetic resonance imaging (MRI) that is more sensitive than mammography (Dixon, 2006).

Lobular carcinoma in situ (LCIS) arises in milk glands, and generally occurs before the menopause. This type of carcinoma it is hard to detect in mammography

`

and when the woman does palpation. May be due to the difficulty to diagnosis LCIS, between 25 and 20% of women presenting this kind of tumor develop an invasive breast cancer (Dixon, 2006). There exist other types of breast carcinomas, but with lower incidence, such as inflammatory breast carcinoma (IBC) and Paget's disease. Inflammatory breast carcinoma, Figure 5, are uncommon and characterized by brawny, redness, warmth, swelling, and erythematous skin changes and have the worst prognosis of all locally advanced breast cancers.

Figure 2.2. Inflammatory breast carcinoma (Dixon, 2006)).

The IBC is produced by dermal lymphatic obstruction, and the diagnosis of this kind of cancer is done in advanced stages. The survival to this carcinoma it is reduced to 25-50 % after five years of evolution, due to an existence of the early lymphatic invasion (Dixon, 2006; Jatoi, 2010). Paget's disease consists in a chronic eczematoid lesion of the nipple associated with an underlying breast malignancy. This disease can be due to a carcinoma in subareolar ducts (Dixon, 2006).

2.3. Mammography :

`

Mammography is the most commonly used technique to detect breast cancer at early stages, usually pre-symptomatic. When symptoms are developed, the cancer has typically become invasive and consequently the prognosis is less favorable (Oliver, 2010). This technique aim is to assist the radiologist to reduce missed breast lesion detection and consequently prevent the propagation of the cancer in to a more severe stage.

2.3.1Mammography Equipment:

Mammography is an imaging procedure for examination of the breast that gives information about breast morphology, anatomy and pathologies, is used for detection and diagnosis of breast cancer, as well as evaluates mass lesions in breast. The early detection of breast cancer is an important factor to treat this disease with success.

This procedure is similar to the other X-Rays, however, are used low doses, presenting a high quality that leads to high contrast and resolution and low noise (Sivaramakrishna, Gordon, 1997). The breast is sensitive to ionizing radiation, so it is desirable to use the lowest radiation dose compatible with excellent image quality.

Mammography is more sensitive and specific in assessing fatty breasts than dense breast. Dense breast tissue is particularly difficult to assess in young women. Mammography is also used in assisting needle core biopsies and for localization of non-palpable lesions (Chinyama, 2000). In screening mammography the uniform compression of the breast is important to ensure image contrast, thus these tools have to be highly sensitive, identifying as correctly as possible those tumors that could be malignant. On the other hand, diagnostic mammography is usually more time consuming, expensive and provides higher radiation dose to the patient that screening mammography, so diagnostic tools must have a great specificity in order to really detect those tumors that are malignant (Perez, 2002).

`

In order to assess differences in density between the breast tissue image acquisition is done using two views: a cranio caudal (CC) and mediolateral oblique (MLO). Generally, on MLO view, more breast tissue can be projected than on the CC view because of the slope and curve of the chest wall. On CC projection, Figure 6a, must be included all breast tissue with the exception of the axillaries portion. During the positioning is important to make sure that is included the upper and posterior breast tissue, through the elevation of breast within the limit of its natural mobility. The projection MLO, Figure 6b, should include as much breast tissue as possible. The image should include the free margin of the pectoralis major muscle to ensure that the patient is as far over the detector as possible and that the tail of the breast is imaged (Kopans, 2007).

(a) (b)

Figure 2.3. Two distinct mammographic projections: a) Cranio Caudal view; b) Medio Lateral Oblique view (from (Kopans, 2007)).

`

Once localized lesions are needed methods for divided the breast in small areas. The method of the quadrants divides the breast using the nipple as reference. Figure 2.4 shows two forms of represent this method.

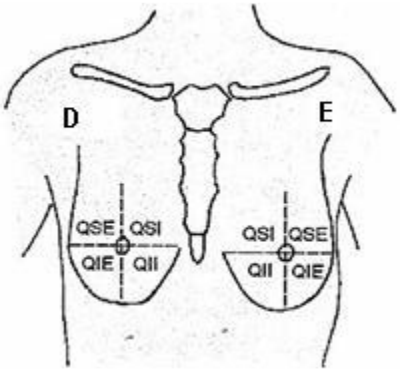

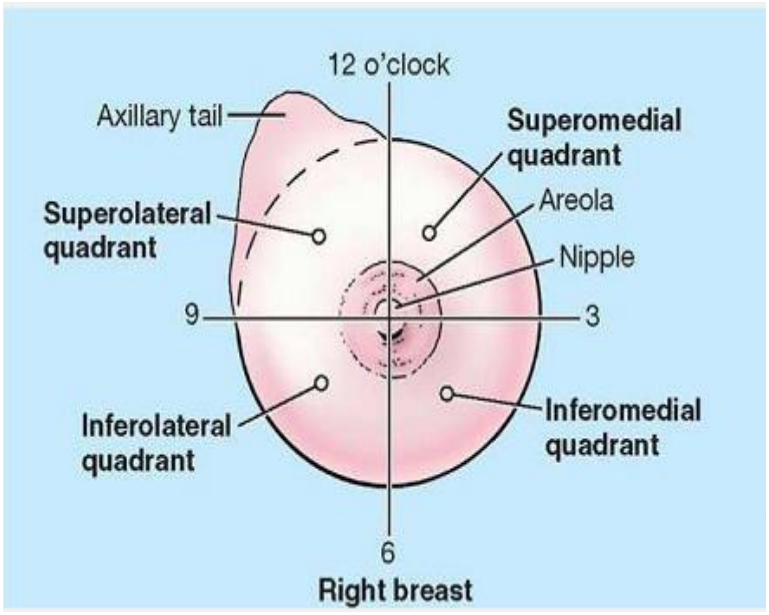

(a) **(b)**

Figure2.4. – Breast localization: a) quadrants method; b) nomenclature of each quadrant (from (Kopans, 2007; Moore&Agur, 2003)).

The essential components of the mammographic imaging system are a mammographic X-ray tube, a device for compressing the breast, an anti-scatter grid, a mammographic image receptor, and an automatic exposure control (AEC), as shown in Figure 2.5.

`

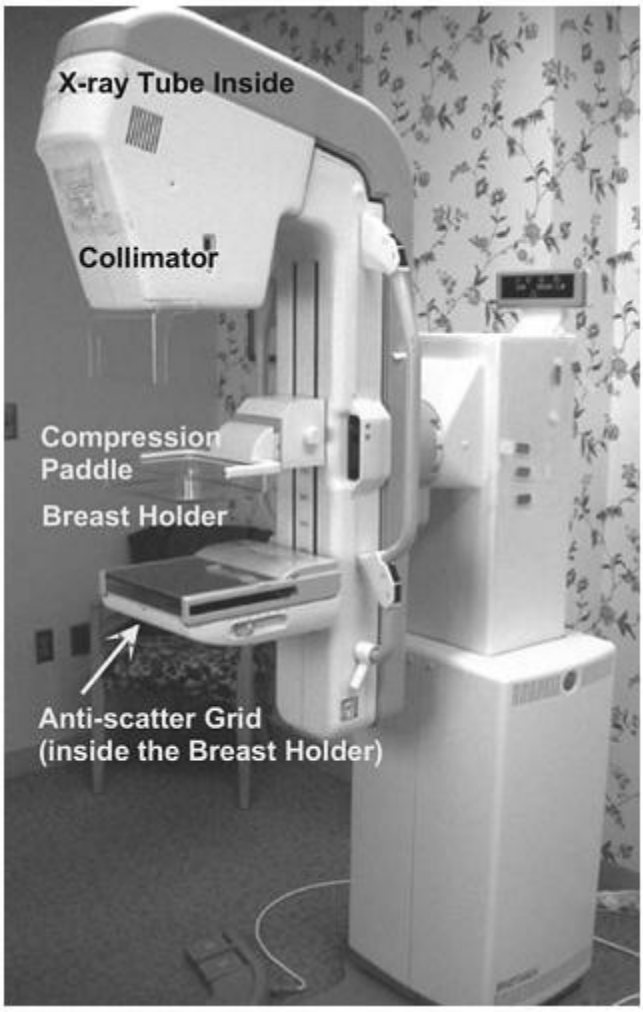

Figure 2.5. – A typical mammography unit (from (Akay, 2006)).

2.3.2. X-ray:

tube An important difference in mammographic tube operation compared with conventional radiographic tube operation is the low operating voltage, typically below 35 kVp. The X-ray tubes are formed by a glass ampoule under vacuum, where there is an internal filament, a cathode and a target, the anode, having a window through which passes the useful beam. The electric current passing through the cathode produces electrons that are accelerated by the potential difference between cathode and anode (Akay, 2006). The voltage applied to cause

`

the potential difference between cathode and anode, determines the maximum photon energy which will be transmitted for the breast. So, it is necessary the existence of a collimator and filters to limit and direct the output of radiation. The low voltages applied in the tube, there will cause a reduction in the energy beam produced, also reducing the dose received by the patient. The focus used to establish the image is provided by two filaments contained in the x-ray tubes, the large focus with 0.3 mm and the thin focus with 0.1 mm. These filaments must be made of a material having a high melting, usually made of tungsten, molybdenum or rhodium (Webster, 2006).

2.3.3Compression Unit:

During the image acquisition process, it should be avoided the loss of resolution caused by the patient movement, for that the patient must be hold breath, using the lowest exposure time possible and immobilizing the breast by compression. As seen previously, the uniform compression decreases the thickness of breast, allowing a better penetration of the X-ray beams. This procedure minimizes superimposition and geometric unsharpness, while resolution is improved as the distance to the object of interest is decreased. Furthermore, it is important to ensure that the area of concern is included in the field of view, because lesions can “roll” or “squeeze” out. It also improves the image contrast and minimizes superposition from different plans (Bronzino, 2000).

2.3.4. Anti-Scatter Grid:

These grids are composed of linear lead (Pb) separated by a rigid interspace material and placed between the breast holder and the cassette slot. The absorption grid is projected with adequate width and spacing with the purpose of absorbing mainly the scattered radiation without interfering on primary radiation. Anti-scatter grids are used to avoid an image contrast decrease produced by scattered radiation

`

when reaches the image receptor. The static grids have thin slices with a low resolution compared with the system in order to not to be displayed in the image (Akay, 2006).

2.3.5. Image Receptor:

The fluorescents screens in conjunction with single coated radiographic film allow that Xrays pass through the cover of a light-tight cassette and the film to impinge upon the screen. The cassettes guarantee a good contact between the screen and film. The crystals absorb the phosphor energy and produce light with an isotropic distribution. Higher sensitization of the film velocities is related to reducing the radiation dose to the patient. However, faster films tend to be noisier. The sensitization velocity is related to the film thickness; thinner films tend to be slower, but have better resolution. More recent films in mammography have higher qualities resolution, velocity and low noise. However, the scattering of light from the fluorescents screens reduces the resolution of the system. The radiographic films needs of chemical processes that absorb most of the light and display the image (Bronzino, 2000).

2.3.6. Automatic Exposure Control (AEC):

These devices of AEC compensate automatically the variations of absorption generated by the breast anatomy, reducing the final dose of radiation and avoiding repetitions. The sensors allow conjugate time exposure with the density and thickness of the tissues (Akay, 2006).

2.3.7. Noise:

The doses in mammography are kept as low as possible because of health effects. However, X-ray quantum noise becomes more apparent in the image as the dose is lowered. This noise is due to the fact that there is an unavoidable random variation in the number of x-rays reaching a point on an image detector. The quantum noise

`

depends on the average number of X-rays striking the image detector and is a fundamental limit to radiographic image quality. The granularity of the film is another source of noise and increases the higher the speed of film used. Hence, there is a necessity to adjust the speed to maintain a high image quality. The grain of the film is finite in size, and if the film image is enlarged, the inhomogeneity of the film grain becomes apparent (Bronzino, 2000). In mammography, high image quality is essential because most of the relevant information of the mammogram corresponds to small details, such as microcalcifications, which can only be identified with a high spatial resolution image (Akay, 2006).

2.3.8. Digital Mammography:

Digital mammography is the most recent significant development in mammography, which uses essentially the same conventional mammography system, but the screen film system is replaced by a detector, which produces an electronic signal that is digitized and stored, Figure 9. This technique has many practical advantages over film-screen mammography (FSM), but only when its performance reaches the standards of FSM this new technology can be fully justified. Screening mammography has been shown to be effective in reducing breast cancer mortality. Full field digital mammography (FFDM) is increasingly used in the clinical setting, with a number of advantages resulting in better detection of breast cancer. With FFDM, the processes of image acquisition, processing, and display are decoupled or separated. This allows for optimization of each process (Bluekens, 2010).

`

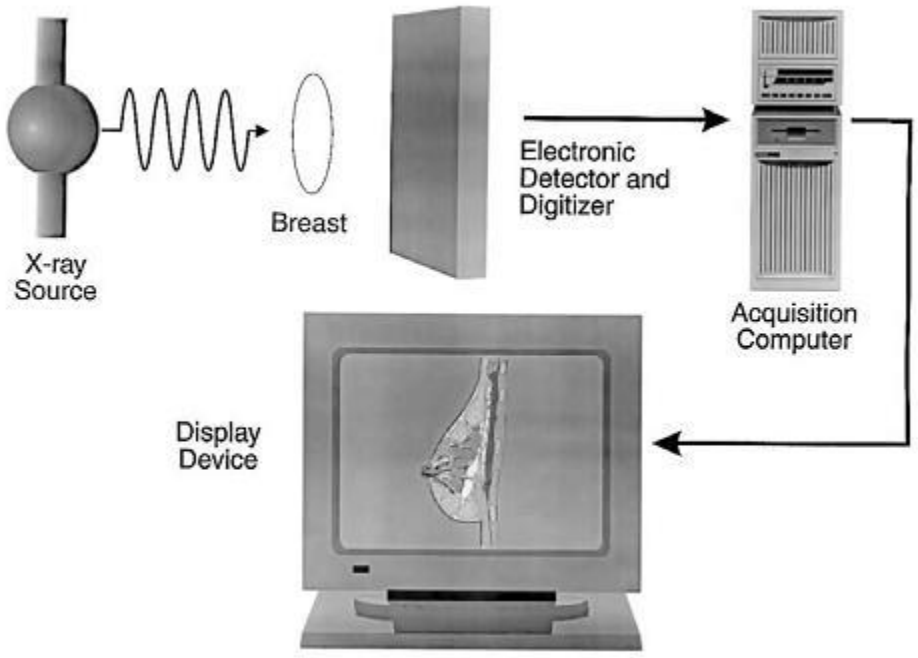

Figure 2.6. – Schematic representation of a digital mammography system (from (Bronzino, 2000)).

In digital mammography, some of the limitations of FSM are overcome. The detected X-ray photons are converting directly to numeric values. The digital images can be processed by a computer, displayed in multiple formats, and fed directly to computer aided detection (CAD) software. Moreover, this technique allows the adjustment of the magnification, orientation, brightness and contrast of the image, after the exam (Bronzino, 2000; Tartar, 2008).

Digital images are sampled images, generated instantly after the exposure and have lower noise than SFM because of reduction in quantum mottle and elimination of granular artifacts from film emulsion. Digital mammography provides a broader dynamic range of densities and greater contrast resolution in dense breasts (Nees, 2008).

In image processing, the contrast and brightness may be changed and enlarge part or entire breast. Post-acquisition processing may compensate for problems of

`

underexposure or over exposure. Image display systems for diagnosis include one or more high resolution monitors, a computer and image display software. For interpretation of image annotation and measurement tools are available, including linear, area and angle measurements. Sometimes, it is important to invert the gray-scale used for a better view of microcalcifications. Digital storage is able to store images in DICOM, it allows a rapid mode to access a large amount of data, but that requires a lot of computer memory. It is important that these systems be carefully designed to ensure that data are not lost, and personnel has to be trained to maintain the storage systems and retrieve new data for interpretation and prior exams for comparison (Hashimoto, 2008).

2.4.Texture analysis:

Refers to the branch of imaging science that is concerned with the description of characteristic image properties by textural features. However, there is no universally agreed-upon definition of what image texture is and in general different researchers use different definitions depending upon the particular area of application (Jain, 1998). Texture is defined as the spatial variation of pixel intensities, which is a definition that is widely used and accepted in the field. The main image processing disciplines in which texture analysis techniques are used are classification, segmentation and synthesis. In image classification the goal is to classify different images or image regions into distinct groups. Texture can be defined as a regular repetition of an element or pattern on a surface. Image textures are complex visual patterns composed of entities or regions with sub-patterns with the characteristics of brightness, color, shape, size, etc. An image region has a constant texture if a set of its characteristics are constant, slowly changing or approximately periodic. Texture can be regarded as a similarity grouping in an image (Pietikainen, 2000).

`

2.4.1. Approach to Texture Analysis:

Mathematical procedures to characterize texture fall into Two major categories: - Statistical and Syntactic. Statistical approaches compute different properties and are suitable if texture primitive sizes are comparable with the pixel sizes. These include Fourier transforms, convolution filters, co-occurrence matrix, spatial autocorrelation, fractals, etc. Syntactic and hybrid (Combination of statistical and syntactic) methods are suitable for textures where primitives can be described using a larger variety of properties than just tonal properties; for example shape description. Using these properties, the primitives can be identified, defined and assigned a label. For gray-level images, tone can be replaced with brightness. Statistical methods analyze the spatial distribution of gray values, by computing local features at each point in the image, and deriving a set of statistics from the distributions of the local features. The reason behind this is the fact that the spatial distribution of gray values is one of the defining qualities of texture. Depending on the number of pixels defining the local feature, statistical method can be further classified into first order (one pixel), second-order (two pixels) and Higher-order (three or more pixels) statistics. The basic difference is that first-order statistics estimate properties (e.g. average and variance) of individual pixel values, ignoring the spatial interaction between image pixels, whereas second- and higher order statistics estimate properties of two or more pixel values occurring at specific locations relative to each other. Statistical approaches yield characterizations of textures as fine, coarse etc. Thus one measure of texture is based on the primitive size, which could be the average area of these primitives of relatively constant gray level. The average could be taken over some set of primitives to measure its texture or the average could be about any pixel in the image. If the average is taken within a primitive centered at each pixel in the image, the result can be used to produce a texture image, in which a large gray level at a pixel indicates, First order texture

`

measures are statistics calculated from the original image values, like variance, and do not consider pixel neighborhood relationships Histogram based approach to texture analysis is based on the intensity value concentrations on all or part of an image represented as a histogram. Common features include moments such as mean, variance, dispersion, mean square value or average energy, entropy, skewness and kurtosis. Variance in the gray level in a region in the neighborhood of a pixel is a measure of the texture (Haralick, 1979).

2.4.2.First-order statistics based approach:

First order texture measures are statistics calculated from the original image values, like variance, and do not consider pixel neighborhood relationships

Histogram based approach to texture analysis is based on the intensity value concentrations on all or part of an image represented as a histogram. Common features include moments such as mean, variance, dispersion, mean square value or average energy, entropy, skewness and kurtosis.

Variance in the gray level in a region in the neighborhood of a pixel is a measure of the texture. For example in a 5 X 5 region, the variance is.

$$T_v(x,y) = \frac{1}{25}\sum_{s=-2}^{2}\sum_{t=-2}^{2}|g(x+s,y+t) - \bar{g}|^2$$

where

$$\bar{g} = \frac{1}{25}\sum_{s=-2}^{2}\sum_{t=-2}^{2} g(x+s,y+t)$$

Where s and t are the positional differences in the x, y direction However, the Standard Deviation could also be used instead of variance.

The histogram of intensity levels is thus a concise and simple summary of the statistical information contained in the image. Calculation of the grey-level

`

histogram involves single pixels. Thus the histogram contains the first-order statistical information about the image (or its fragment). Dividing the values $h(i)$ by the total number of pixels in the image one obtains the approximate probability density of occurrence of the intensity levels.

The histogram can be easily computed from the image. The shape of the histogram provides many clues to the characteristics of the image. For example, a narrowly distributed histogram indicated the low-contrast image. A bimodal histogram often suggests that the image contained an object with a narrow intensity range against a background of differing intensity. Different useful parameters (image features) can be worked out from the histogram to quantitatively describe the first-order statistical properties of the image.

Texture analysis based solely on the gray level histogram suffers from the limitation that it provides no information about the relative position of pixels to each other. For example, 2 completely different images each with a 50% black and 50% white pixels (such as a checkerboard and a Salt & Pepper noise pattern) may produce the same gray level histogram. Therefore we cannot distinguish between them using first order statistical analysis (Harlick,1981).

2.4.3.Co-occurrence matrices:

Various statistical approaches for texture representation are Co-occurrence matrices, fractal model, Tamura feature, world decomposition and so on . The co-occurrence matrices are second order statistics to measure texture properties of an input image. Various cooccurrence matrices in the literature are Gray- level cooccurrence Matrix (GLCM) , Gray- level Aura Matrix (GLAM), Gray- level Run Length Matrix (GLRLM), Gray- level Neighbor Matrix (GLNM) (Abraham Chandy, 2014).

`

2.4.3.1.Gray- Level Co-occurrence Matrix (GLCM):

GLCM is second order statistics, which is used to describe the occurrence of combinations of gray level values in an input image with a specified distance and direction. The fig 1(a) represents example of an image with 4 gray levels. The fig 1(b) represents the GLCM of image with a distance 1 unit and direction o◦. Different GLCMs can be generated with four directions, o◦, 45◦,90◦,135◦. These directions are shown in fig 1(c)(Haralick , 1973).

2.4.3.2. Gray Level Aura Matrix (GLAM):

Originally the Aura Matrix was proposed by Elfadel and Picard for modeling texture. An image can be modeled as a rectangular constitution S of m x n grids. Furthermore, consider an image *s* with a neighborhood system N = {N_S, sϵ S} can be defined. At which the neighborhood N_S is built from the basic neighborhood at pixel *s.* The basic neighborhood is there by a chosen structural element. Given two subsets A, B ⊆ S, where |A| is the total number of elements in A.

The aura measure of A with respect to B for neighborhood system *N*, is given as follows

$$m(A, B, N) = \sum_{s\epsilon n} |Ns \cap B|$$

Let N be the neighborhood system over S and {Si, 0 ≤ i ≤ G - 1} be the gray level set of an image over Swith G as the number of different gray levels, then the GLAM of the image g(N) is as follows.

$$g(N) = [a_{i,j}] = [m(s_i, s_j, N)]$$

Where by Si={s ∈ S | xs= i} is the gray level set corresponding to the ith level, and m(Si, Sj, N) is the aura measure of Si with respect to Sj with the neighborhood system N(Zohra & Kamal 2011).

`

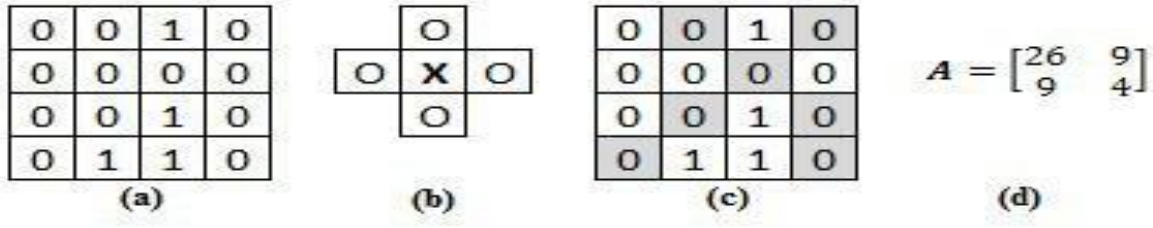

figure 2.7 Process used to create the GLAM

Fig 2.7(a) is a sample binary lattice S, where the subset A is the set of all 1's and B the set of all 0's.Fig 2.7(b) is the structural element of the neighborhood system. Fig 2.7(c) is the shaded sites involved for building m(S 1 ,S 0 ,N). The Fig 2.7 (d) is the corresponding GLAM. The GLAM of an image measures the amount of each gray level in the neighborhood of each gray level. Features are the properties that characterize the texture. Extracted 14 features from the cooccurrence matrix, although in many applications, only 8 (eight) features are widely used, that is: Energy, Entropy, Max Probability, Inverse Diff. Moment, contrast, homogeneity, Inertia, and Correlation. The table Table1 contains thirteen features used to characterize texture in GLCM and in GLAM (Haralick , RM & Dinstein 1973).).

Table 2.1 Textural features:feature used to characterize texture in GLCM and GLAM

S.N 0	Feature Name	Formulate
1	ASM Homogenity	$\sum_{i,j=0}^{N-1} I_i, j^2$
2	Contrast	$\sum_{i,j=0}^{N-1} I_{i,j} (i-j)^2$
3	Local Homogenity	$\sum_{i,j=0}^{N-1} \frac{I_{i,j}}{1+(i-j)2}$

`

4	Correlation	$\sum_{i,j=0}^{N-1} I_{i,j}\left[\frac{(i-\mu_1)(j-\mu_1)}{\sqrt{(\sigma i^2)}(\sigma j^2)}\right]$
5	Dissimilarity	$\sum_{i,j=0}^{N-1} I_{i,j}\,\lvert i-j\rvert$
6	Entropy	$\sum_{i,j=0}^{N-1} I_{i,j}\left(-\log I_{i,j}\right)$
7	Sum of squares	$\sum_{i=0}^{G-1}\{(i-\mu_\rho)*(I(i,j))\}$
8	Difference variance	Variance of $\rho_{x,y}$
9	Information measure of correlation	$\left(1-e^{[-2.0(HXY2-HXY)]}\right)^{\frac{1}{2}}$
10	Information measure of correlation	$\frac{HXY-HXY1}{max\{HX,HY\}}$
11	Difference Entropy	$-\sum_{j=0}^{N-1} I_{x-y(j)}\log\{I_{x-y(j)}\}$
12	Sum Entropy	$\sum_{i=0}^{2N} I_{x-y(i)}\log\{I_{x-y(i)}\}$
13	Sum Average	$-\sum_{i=2}^{2R} iI_{x,y(j)}$

2.4.3.3 GRAY-LEVEL RUN-LENGTH MATRIX (GLRLM):

Like GLCM, GLRLM also used to extract the textural features of the input image. It is mainly based on run length. Run length is the frequency of the neighbors having same gray intensity pixels in same direction. GLRLM is a two dimensional matrix. In GLRLM each element p (k,l/0) is the number of elements l with the

`

grey level value k in the direction 0.The fig 2.8(a) represents a matrix of size 4*4 pixel intensities with 4 gray levels [13]. The fig 2.8(b) shows GLRLM with 0 direction, GLRLM can also be generated in the directions as shown in fig 2.8(c)

1	1	3	4
2	3	1	4
2	2	3	2
3	1	4	1

Fig2.8.a Image of 4 × 4 pixels

Gray level	Run Length(j)			
	1	2	3	4
1	3	1	0	0
2	2	1	0	0
3	4	0	0	0
4	3	0	0	0

Fig.2.8.b. GLRLM Matrix

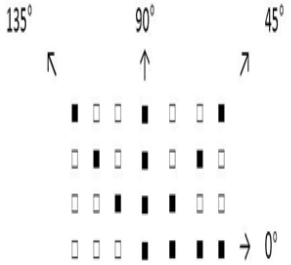

Fig2.8.c. Run Direction

Tang suggests 5 texture features based on this GLRL matrix, namely shot runs emphasis (SRE), long runs emphasis (LRE), gray-level non-uniformity (GLN), run length non-uniformity (RLN), and run percentage (RP). Chu add 2 more features called low gray-level run emphasis (LGRE) and high gray level run emphasis (HGRE). Dasarathy and Holder added 4 more features extracted from the GLRL matrix, namely short-run low gray-level emphasis (SRLGE), short-run high gray-level emphasis (SRHGE), long-run low gray-level emphasis (LRLGE), and long-run high gray-level emphasis (LRHGE) (Chu A,1990).

`

Table2.2 Textural features: Feature used to characterize texture in GLRM

S. No	Features	Formulate
1	Short Run Emphasis(SRE)	$\frac{1}{n}\sum_{i,j}\frac{P(i,j)}{j2}$
2	Long Run Emphasis(LRE)	$\frac{1}{n}\sum_{i,j} j2p(i,g)$
3	Gray Level Non- uniformity(GLN)	$\frac{1}{n}\sum_{i}\left(\sum_{j} P(i,j)\right)2$
4	Run Length Non- uniformity(RLN)	$\frac{1}{n}\sum_{j}\left(\sum_{i} P(i,j)\right)2$
5	Run percentage(RP)	$\sum_{i,j}\frac{n}{P(i,g)j}$
6	Low Gray Level Run Emphasis (LGRE)	$\frac{1}{n}\sum_{i,j}\frac{p(i,j)}{i2}$
7	High Gray Level Run Emphasis (HGRE)	$\frac{1}{n}\sum_{i,j} i2(i,j)$
8	Short-run low gray-level emphasis (SRLGE)	$\frac{1}{n_r}\sum_{i=1}^{M}\sum_{j=1}^{N}\frac{p(i,j)}{i^2,j^2}$
9	Short-run high gray-level emphasis (SRHGE)	$\frac{1}{n_r}\sum_{i=1}^{M}\sum_{j=1}^{N}\frac{p(i,j),i^2}{j^2}$
10	Long-run low gray-level emphasis (LRLGE)	$\frac{1}{n_r}\sum_{i=1}^{M}\sum_{j=1}^{N}\frac{p(i,j),j^2}{i^2}$
11	Long-run high gray-level emphasis (LRHGE)	$\frac{1}{n_r}\sum_{i=1}^{M}\sum_{j=1}^{N} p(i,j),i^2,j^2$

`

2.4.3.4 GRAY LEVEL NEIGHBORS MATRIX (GLNM):

Abraham Chandy et al proposed a statistical matrix, Gray level neighbors matrix (GLNM) in 2014 considering neighbors. The GLNM extracts textural information based on the occurrence of gray level neighbors within the specified neighborhood. The gray level neighbors are the pixels in the specified neighborhood with similar gray level as the centre pixel. In the case of a 3×3 neighborhood, the maximum number ofpossible gray level neighbours is eight. The number of rows and columns of the GLNM are equal to the number of gray levels and maximum gray level neighbours, respectively. If the number of gray levels and the neighbourhood size are larger it may result in an array of larger dimension, which can be controlled to a considerable extent by reducing the quantization level of the image. The matrix element (i, j) of the GLNM is the 'j' number of neighbours within the given neighbourhood having the intensity 'i', which is defined as

$$G(i,j) = \#[(x,y)](x,y) = i, \#\left[(p,q)|N_{x,y}(p,q) = i\right] = j$$

where, # denotes the number of elements in the set and $N_{x,y}(p,q)$ is the defined neighbourhood in the image. The construction of GLNM matrix is shown in Fig. 2.9. Fig.2.9(a) contains a 6×6 image matrix with eight gray levels ranging from0 to 7. Figure 2.9(b) shows the corresponding GLNM generated. Fig.2.9 (c) shows the different occurrences of 2neighbors of zero as center pixel (Abraham ,(2014))

`

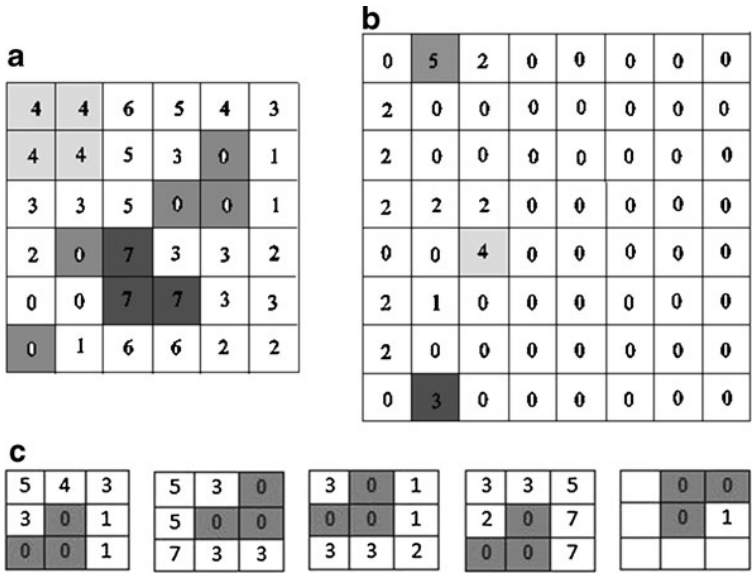

Fig2. 9(a) image matrix (b) GLNM (c)Illustration of generating the value of G (1,2)

Table 2.3. Textural featuresFeature used to characterize texture in GLNM

S. No	Feature	Formulae
1	Feature1, F1	$\sum_{i=1}^{N_1}\sum_{j=1}^{N_1}\{G(i,j)\}^2$
2	Feature2, F2	$\sum_{n=0}^{N_1-1} n^2 \left(\sum_{\lvert i-j\rvert=n} G(i,h) \right)$
3	Feature3, F3	$\sum_{i=1}^{N_1}\sum_{j=1}^{N_1}\frac{G(i,j)}{1+(i-j)^2}$
4	Feature4, F4	$\sum_{j=1}^{N_1}\left(min_j-\mu\right)^2 G(i,j)$ $\mu=\frac{1}{N_z\times N_n}\sum_{i=1}^{N_1}\sum_{j=1}^{N_1}G(i,j)$

`

2.5. Previous study:

Gar elnabi1 et.al (2011) in this study was use image-processing techniques to characterize the normal breast tissues. Clustering techniques was developed to classify the breast tissue into one of 5 different tissue types including fat, glandular, connective, dense tissues and pectoral muscle. The classification was achieved by using a novel technique involving a subset of the elements (the values on the diagonals) in the Spatial Grey Level Dependence (SGLD) matrix which was calculated using texture features, thus it was called the diagonal SGLD method (dSGLD). The ultimate goal of this study was therefore to design and implement a computerized characterization method that mimics the radiologist's characterization of tissue composition in digitized mammograms. The classification results using dSGLD and SGLD features achieved an accuracy of 80 % and 71%, respectively when compared to radiologists' classifications.

Rinku Rabidas (2016.) in this study was develop a comparative analysis of different texture features based on local operator has been produced for the determination of mammographic masses as benign or Binary Pattern (LBP), LBP Variance (LBPV), and Completed LBP (CLBP) descriptors are extracted to evaluate their potential for mass classification in a Computer-Aided Diagnosis (CAD) system. An *Az* value of 0.97 ± 0.02 and an accuracy of 92.25 ± 0.01% have been achieved, while experimenting on 200 mass cases from the DDSM database, by selecting the optimal set of features employing stepwise logistic regression method, followed by classification via Fisher Linear Discriminant Analysis (FLDA) using 10-fold cross validation.

M. Abdalla.et.al. (2011). studying the detection of breast tumors, there has been great attention to the modern textural features analysis of breast tissues on mammograms. Detecting of masses in digital mammogram based on second order statistics has not been investigated in depth. During this study, the breast cancer

`

detection was based on second order statistics. The extraction of the textural features of the segmented region of interest (ROI) is done by using gray level co-occurrence matrices (GLCM) which is extracted from four spatial orientations; horizontal, left diagonal, vertical and right diagonal corresponding to (0o, 45o, 90o and 135o) and two pixel distance for three different block size windows (8x8, 16x16 and 32x32) . The results show that the GLCM at 0o, 45o, 90o and 135o with a window size of 8X8 produces informative features to classify between masses and non-masses. Our method was able to achieve an accuracy of 91.67% sensitivity and 84.17% specificity which is comparable to what has been reported using the state-of-the-art Computer-Aided Detection system.

K. Vaidehi, T. S. Subashini (2014) this study the aim to develop an automated breast mass characterization system for assisting the radiologist to analyze the digital mammograms. Mammographic Image Analysis Society (MIAS) database images are used in this study. Fuzzy C-means technique is used to segment the mass region from the input image. GLCM texture features namely contrast, correlation, energy and homogeneity are obtained from the region of interest. The texture features extracted from gray level co-occurrence matrix (GLCM) are computed at distance d=1 and θ=0°, 45°, 90°, 135°. These with three classifiers namely adaboost, back propagation, neural network and sparse representation classifiers are used for characterizing the region containing either benign mass or malignant mass. The experimental results show the SRC classifier is more effective with an accuracy of 93.75% and with the Mathew's correlation coefficient (MCC) of 87.35%.

Berkman Sahiner. (1998) develops new rubber band straightening transform (RBST) is introduced for characterization of mammographic masses as malignant or benign. The RBST transforms a band of pixels surrounding a segmented mass onto the Cartesian plane the (RBST) image. The border of a mammographic mass

`

appears approximately as a horizontal line, and possible spiculations resemble vertical lines in the RBST image. In this study, the effectiveness of a set of directional texture features extracted from the RBST images was compared to the effectiveness of the same features extracted from the images before the RBST. A database of 168 mammograms containing biopsy-proven malignant and benign breast masses was digitized at a pixel size of 100 mm3100 mm. Regions of interest (ROIs) containing the biopsied mass were extracted from each mammogram by an experienced radiologist. A clustering algorithm was employed for automated segmentation of each ROI into a mass object and background tissue. Texture features extracted from spatial gray-level dependence matrices and run-length statistics matrices were evaluated for three different regions and representations :(i) the entire (ROI); (ii) a band of pixels surrounding the segmented mass object in the (ROI); (iii) and the RBST image. Linear discriminant analysis was used for classification, and receiver operating characteristic (ROC) analysis was used to evaluate the classification accuracy. Using the ROC curves as the performance measure, features extracted from the RBST images were found to be significantly more effective than those extracted from the original images. Features extracted from the RBST images yielded an area (*Az*) of 0.94 under the ROC curve for classification of mammographic masses as malignant and benign.

Shi et al. (2008) this study was to develop an automated method for mammographic mass segmentation and explore new image based features in combination with patient information in order to improve the performance of mass characterization. Previous CAD system, which used the active contour segmentation, and morphological, textural, and speculation features, has achieved promising results in mass characterization. The new CAD system is based on the level set method, and includes two new types of image features related to the presence of micro calcifications with the mass and abruptness of the mass margin,

`

and patient age. A linear discriminate analysis (LDA) classifier with stepwise feature selection was used to merge the extracted features into a classification score. The classification accuracy was evaluated using the area under the receiver operating characteristic curve. Our primary data set consisted of 427 biopsy-proven masses (200 malignant and 227 benign) in 909 regions of interest (ROIs) (451 malignant and 458 benign) from multiple mammographic views. Leave-one-case-out resembling was used for training and testing. The new CAD system based on the level set segmentation and the new mammographic feature space achieved a view-based as value of 0.83±0.01. The improvement compared to the previous CAD system was statistically significant (p=0.02). When patient age was included in the new CAD system, view-based and case based as values were 0.85±0.01 and 0.87±0.02, respectively. The performance of the new CAD system was also compared to an experienced radiologist's likelihood of malignancy rating. When patient age was used in classification, the accuracy of the new CAD system was comparable to that of the radiologist (p=0.34). The study also demonstrated the consistency of the newly developed CAD system by evaluating the statistics of the weights of the LDA classifiers in leave one-case-out classification. Finally, an independent test on the publicly available digital database for screening mammography (DDSM) with 132 benign and 197 malignant ROIs containing masses achieved a view-based as value of 0.84±0.02.

Sharma et.al (2013). Breast tissue density has been shown to be related to the risk of development of breast cancer, since dense breast tissue can hide lesions, causing the disease to be detected at later stages. Thus there is a need for the development of efficient techniques for the classification of breast density. In the proposed work, breast density (Fatty and Dense) is used as a pattern for classification. For carrying out the experiments mini-MIAS database has been used. This database contains images from screening mammography and has been widely used in the

`

recent research. Texture features based on Grey Level Difference Statistics and Fourier Power Spectrum has been used for representing the texture pattern of fatty and dense mammograms. These features are then subsequently fed to the SVM classifier to classify fatty and dense mammograms. The results show that the extracted features perform very well with Polynomial Kernel of Support Vector Machine (SVM) classifier giving an accuracy of 97.25%. The experimental results encourage the use of proposed method for the classification of breast density.

`

Chapter Three
Methodology

3.1. Mammography Machine used:

Table 3.1. shows the feature of the mammography machine center used.

Specification	**Machine1**	**Machine2**	**Machine3**
Model	NM-GA	Liyum	Mammomat
Manufacturer	Neusoft medic system	Corman (Italy)	SIEMENS
Serial No	G-A-15060003	1 Lil Hf P/ 231/co	55643
Manufacture date	June 18 2015	May 2009	2004
Power supply	220- 250 volt 50/6 Hz	220-240 volt 50/60 H	380-480 volt 59/60 H

3.2. IDL software:

IDL is vectorized, numerical, and interactive, and is commonly used for interactive processing of large amounts of data (including image processing). The syntax includes many constructs from Fortran and some from C.

IDL originated from early VAX/VMS/Fortran, and its syntax still shows its heritage:

```
x = findgen(100)/10
y = sin(x)/x
plot,x,y
```

`

The findgen function in the above example returns a one-dimensional array of floating point numbers, with values equal to a series of integers starting at 0.

Note that the operation in the second line applies in a vectorized manner to the whole 100-element array created in the first line, analogous to the way general-purpose array programming languages (such as APL, J or K) would do it. This example contains a divide by zero; IDL will report an arithmetic overflow, and store a NaN value in the corresponding element of the y array (the first one), but the other array elements will be finite. The NaN is excluded from the visualization generated by the plot command.

As with most other array programming languages, IDL is very fast at doing vector operations (sometimes as fast as a well-coded custom loop in Fortran or C) but quite slow if elements need processing individually. Hence part of the art of using IDL (or any other array programming language, for that matter) for numerically heavy computations is to make use of the built-in vector operations (Schienle, Mike1991).

3.3. Methods:

Patient was selected according to the study variability and mammography images was performed for two group of patient which those with breast mass after confirmation by biopsy and compared to patient with normal breast tissue(fat, glandular and connective tissue) in mammogram images . The primary image was converted into jpg format as an input image for IDL image processing program Then the images were read by IDL and firstly textural features that represent the first order were extracted from the Breast tissue from the two groups which are the breast with mass and normal breast tissue(fat, glandular and connective tissue) , these features include mean, standard deviation and energy and secondly textural features that represent the higher order were extracted from the Breast tissue from

`

the two groups and these feature included 6 Grey-level run-length matrix GLRLM features (LRE, GLN, RLN, RP, HGLRE and LRHGLE).using a window of 3×3 pixel from all data set using breast and as Region of Interest (ROI) through an algorithm written in Interactive Data Language (IDL) software . The extracted features were classified using stepwise linear discriminant analysis using breast as separate data set where each include the previous two groups; in order to find the most discriminant textural feature in each set as well as the classification accuracy and sensitivity concerning the characteristics of each set.

3.4 Technique used:

The breast is compressed using a dedicated mammography unit. Parallel-plate compression evens out the thickness of breast tissue to increase image quality by reducing the thickness of tissue that x-rays must penetrate, decreasing the amount of scattered radiation (scatter degrades image quality), reducing the required radiation dose, and holding the breast still (preventing motion blur). In screening mammography, both head-to-foot (craniocaudal, CC) view and angled side-view (mediolateral oblique, MLO) images of the breast are taken. Diagnostic mammography may include these and other views, including geometrically magnified and spot-compressed views of the particular area of concern. Deodorant, talcum powder or lotion may show up on the X-ray as calcium spots, so women are discouraged from applying them on the day of their exam. There are two types of mammogram studies: screening mammograms and diagnostic mammograms. Screening mammograms, consisting of four standard X-ray images, are performed yearly on patients who presents with no symptoms. Diagnostic mammograms are reserved for patients with breast symptoms, changes, or abnormal findings seen on their screening mammograms.

`

3.5 Design of the study:

This study is analytical-case control type deals with mass of breast and normal breast tissue(fat, glandular and connective tissue).

3.6 Population of the study:

The population of this study consisted of two groups of patient, those with normal breast free from any mass, group two patients having breast mass.

The study includes female with their age ranged from 27 years to 80years old

3.7 Sample size and type:

This study consisted of 155 patients having breast mammography examination, referred to mammography department for scanning. Patients were selected conveniently.

3.8 Place and Duration of the study:

This study was carried out in the period from May 2016 to August 2020 in radiology department in Alzaytoua Specialist Hospital, Advanced Diagnostic Centre in Bahrie and Modern Medical Centre

3.9 Inclusion criteria:

All patients with breast mass who have mammographic images and FNAC.

3.10 Exclusion criteria:

All patients undergoing surgical resection of the breast mass, patient without FNAC biopsy.

3.11Data analysis:

The data discriminated by using SW-LDA in SPSS technique in order to select the most significant feature that used to classify breast mass and breast tissue (fat, connective and glandular) and excels Microsoft office was also used.

`

3.11Ethical approval:

The ethical approval was granted from the hospital and the radiology departments; which include commitment of no disclose any information concerning the patient identification as well as consent from the patients.

`

Chapter Four

Results

4.1 feature extraction by using first order statistics:

Feature extracted from mammogram images by using first order statistics a set of 3 histogram feature (Mean, standard deviation and energy), discriminated analysis used and the result was:

Table 4.1. a confusion matrix shows the classification accuracy of the original classes versus the predicted membership according to linear discriminant functions [multiple linear regression equation]

Classes		***Predicted Group Membership***				***Total***
%	***Original Group***	***Tumor***	***Gland***	***Fat***	***Connective T***	
	Tumor	***96.8***	***.0***	***.0***	***3.2***	***100.0***
	Gland	***42.1***	***57.9***	***.0***	***.0***	***100.0***
	Fat	***.0***	***.0***	***98.9***	***1.1***	***100.0***
	Connective T	***.0***	***.0***	***1.5***	***98.5***	***100.0***

94.0% of original grouped cases correctly classified

Table4.1 show classification score matrix generated by linear discriminate analysis and the overall classification accuracy of breast masses and breast tissue 94.0%, were the classification accuracy of gland 86.8%, fat 98.2%, connective tissue 98.9%, While the tumor showed a classification accuracy 98.5%.

`

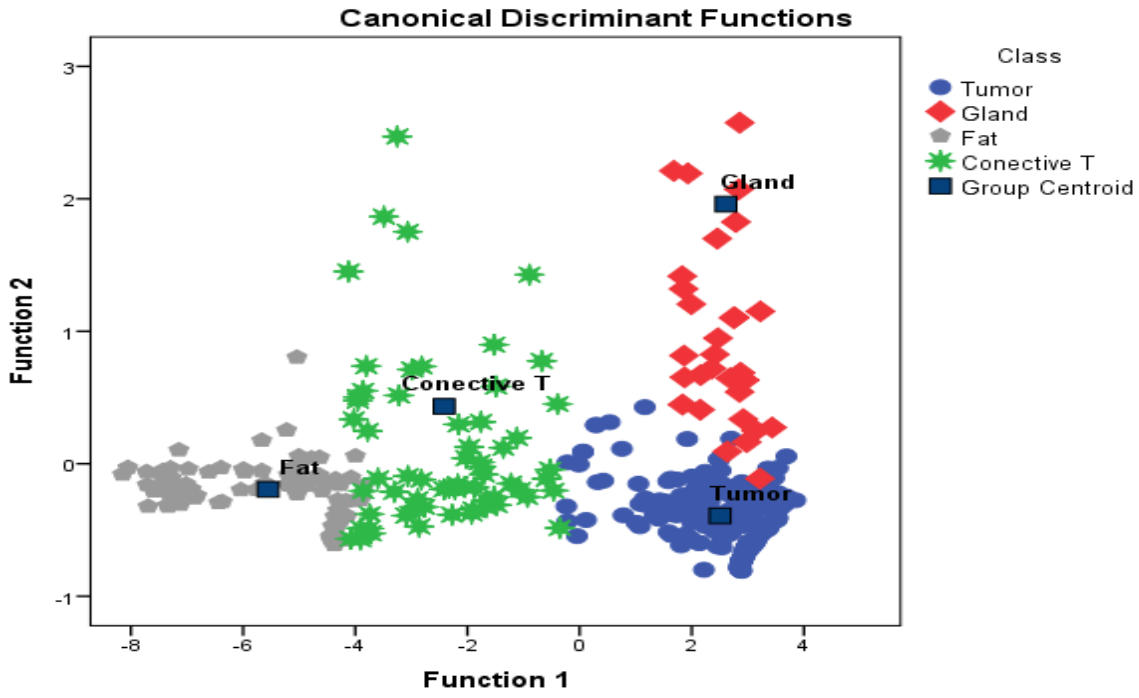

Fig 4.1 scatter plot demonstrates the distribution of four Classes according to their textural feature using linear discriminate analysis functions

the classification showed that the breast tissues was classified well from the rest of the tissues although it has characteristics mostly similar to surrounding tissue.

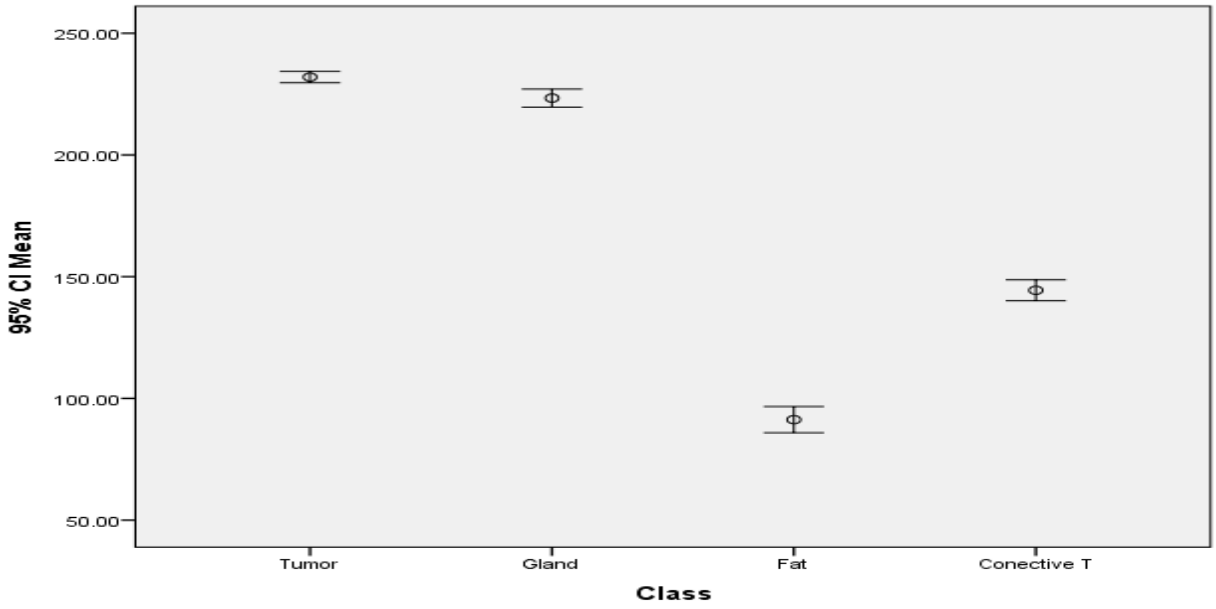

`

Fig .4.2 show error bar plot for the CI mean textural features that selected by the linear stepwise discriminate function as a discriminate between all features. From the discriminate power point of view in respect to the applied features the mean can differentiate between all the classes successfully.

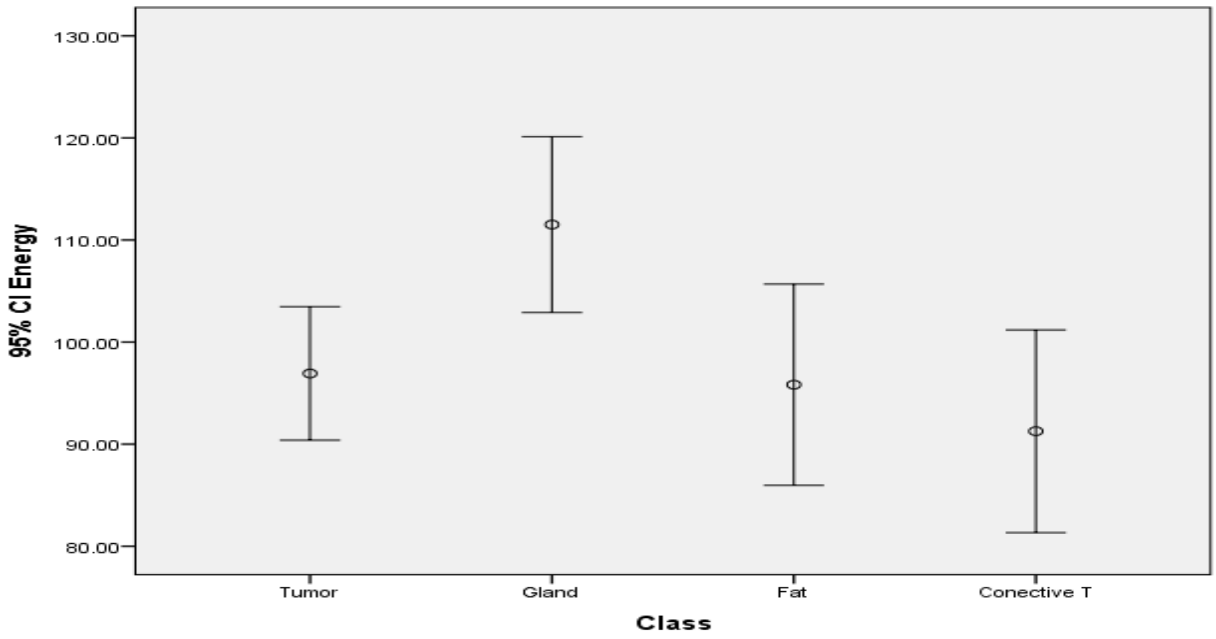

Fig 4.3.show error bar plot for the CI energy textural features that selected by the linear stepwise discriminate function as a discriminate feature where it discriminates between all features.

`

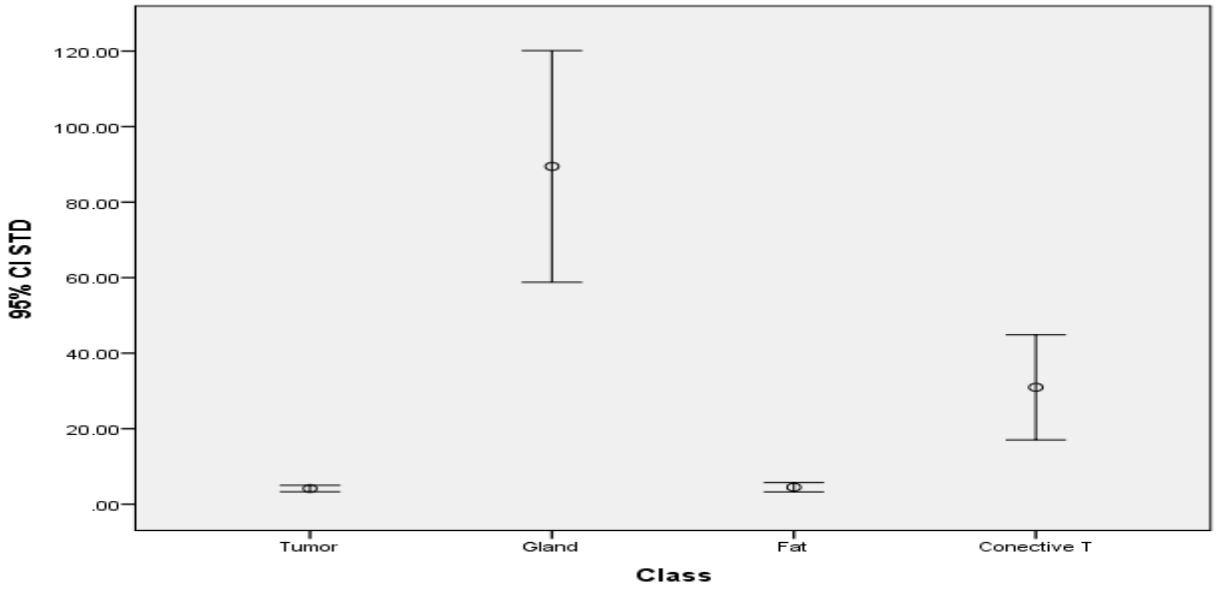

Fig 4.4 show error bar plot for the CI standard deviation textural features that selected by the linear stepwise discriminate function to discriminates between all features. From the discriminate power point of view in respect to the applied features the STD can differentiate between all the classes successfully.

4.2 Feature extraction by using higher order statistics:

Feature extracted from 155 mammogram images by using a set of 6 gray-Level run –Length matrix (GLRLM) features are (long run emphasis) (LRE), grey level non uniformity (GLN), run length non uniformity (RLN),) Run percentage (RP), High Gray Level Run Emphasis(HGLR)E and Low Gray Level Run Emphasis (LRHGLE), discriminated analysis used and the result was:

Table 4.2. a confusion matrix shows the classification accuracy of the original classes versus the predicted membership according to linear discriminant functions.

%	***Original Group***	***Tumor***	***Gland***	***Fat***	***Connective T***	

`

	Tumor	***88.9***	***.0***	***.0***	***.0***	***100.0***
	Gland	***.0***	***98.9***	***.0***	***.0***	***100.0***
	Fat	***.0***	***.0***	***86.3***	***.0***	***100.0***
	Connective T	***.0***	***.0***	***1.5***	***91.9***	***100.0***

91.5% of original grouped cases correctly classified

Table 4.2. show classification score matrix generated by linear discriminate analysis and the overall classification accuracy of breast masses 91.5%, were the classification accuracy of gland 98.9%, fat 86.3%, connective tissue 91.9%, While the tumor showed a classification accuracy 88.9%.

`

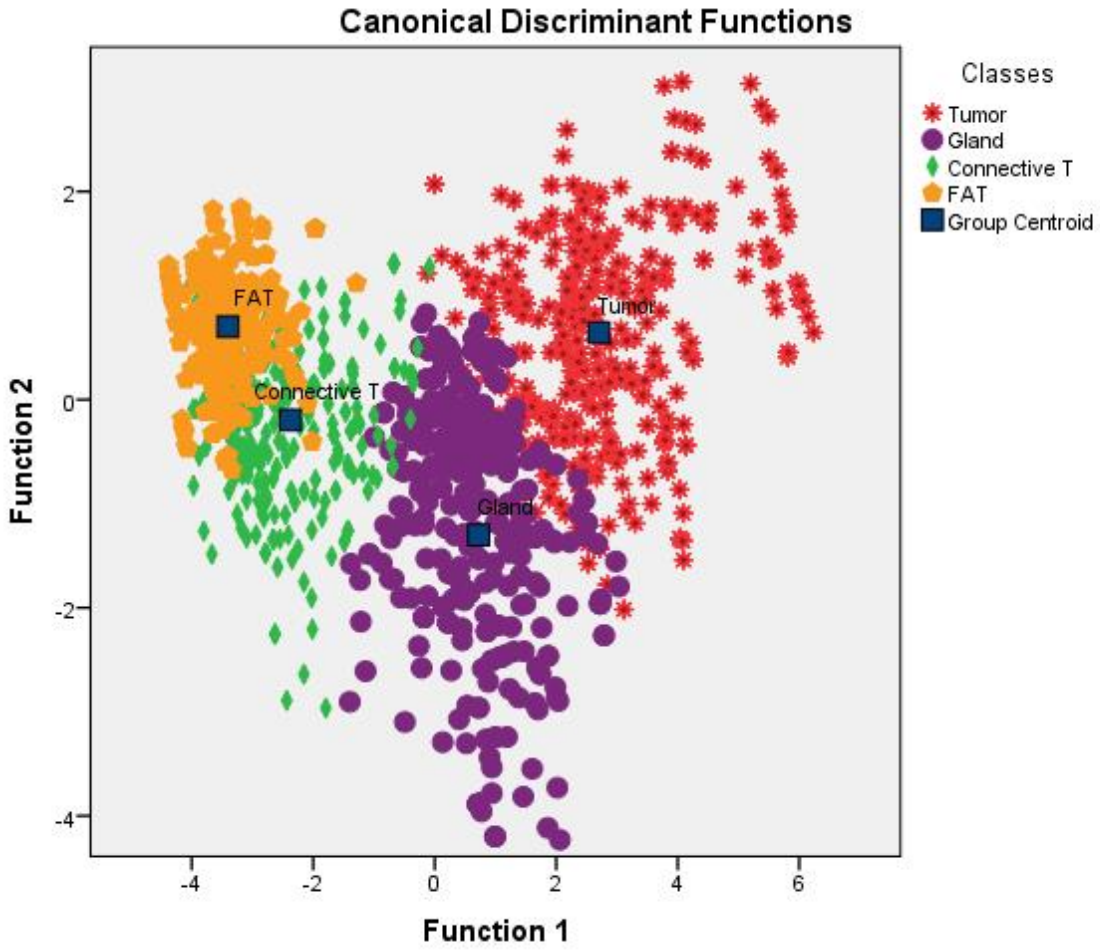

Fig 4.5. scatter plot demonstrates the distribution of four Classes according to their textural feature using linear discriminate analysis functions

the classification showed that the breast tissues was classified well from the rest of the tissues although it has characteristics mostly similar to surrounding tissue.

`

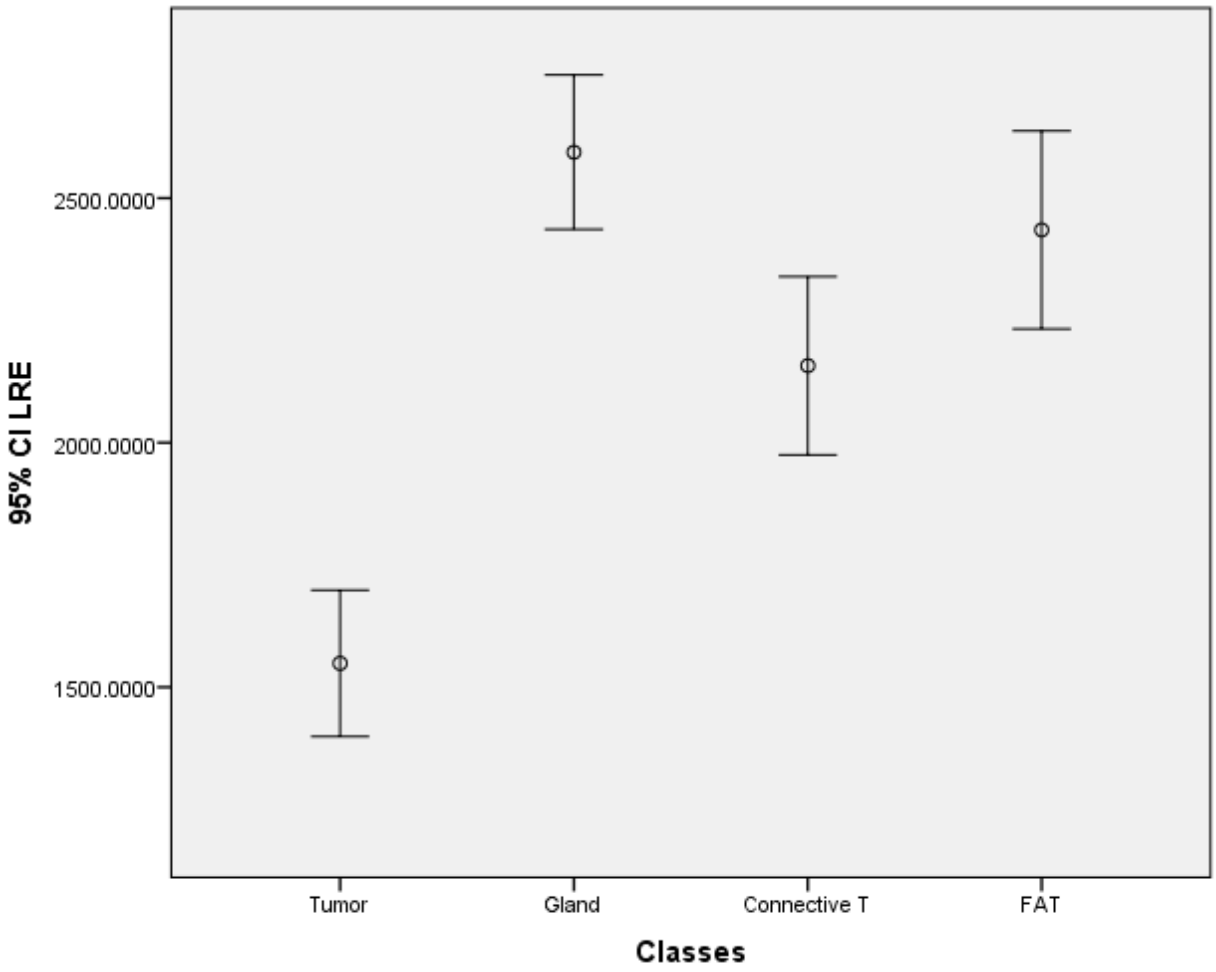

Fig .4.6. show error bar plot for the CI LRE textural features that selected by the linear stepwise discriminate function as a discriminate between all features. From the discriminate power point of view in respect to the applied features the LRE can differentiate between all the classes successfully.

`

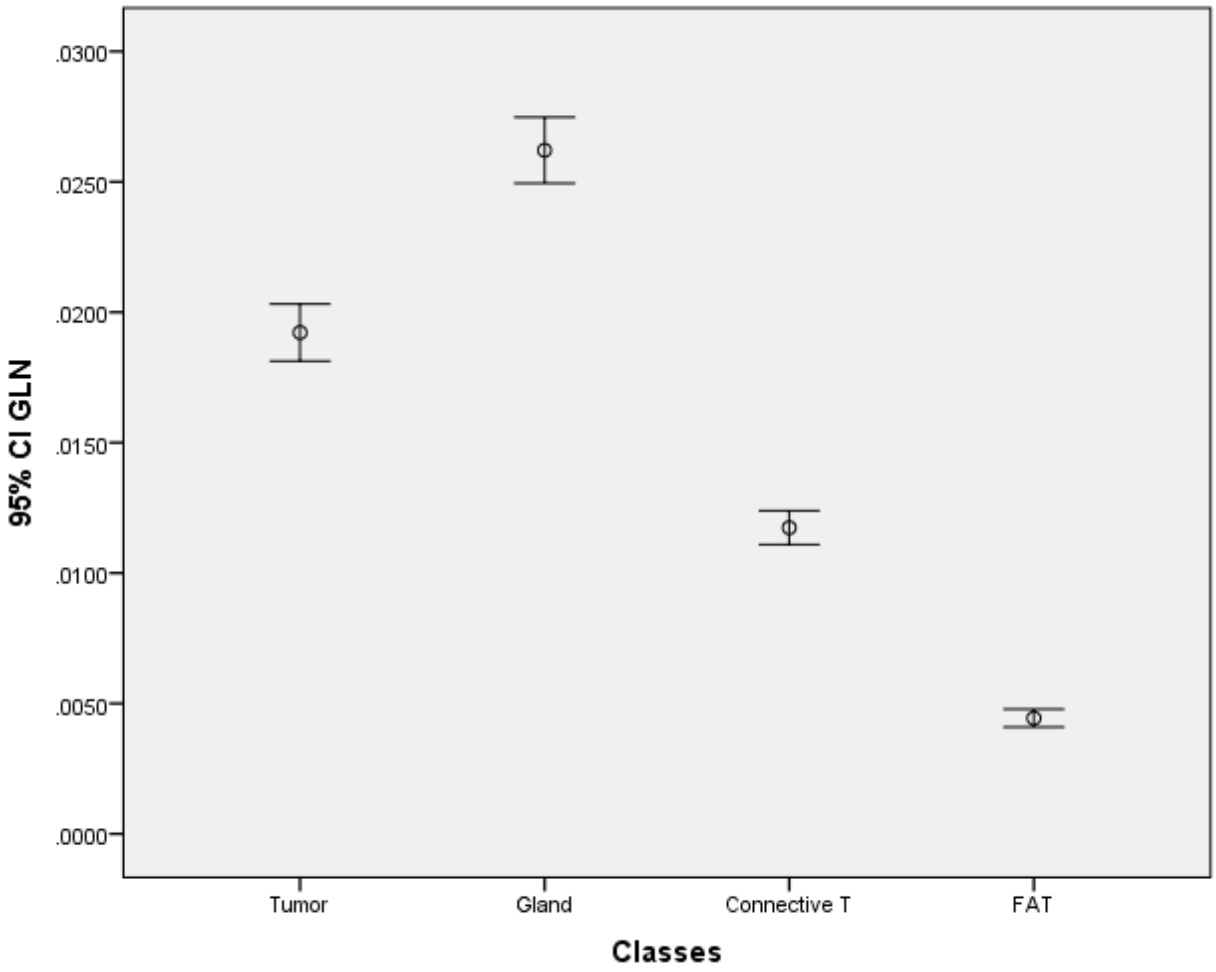

Fig 4.7. show error bar plot for the CI GLN textural features that selected by the linear stepwise discriminate function as a discriminate feature where it discriminates between all features.

`

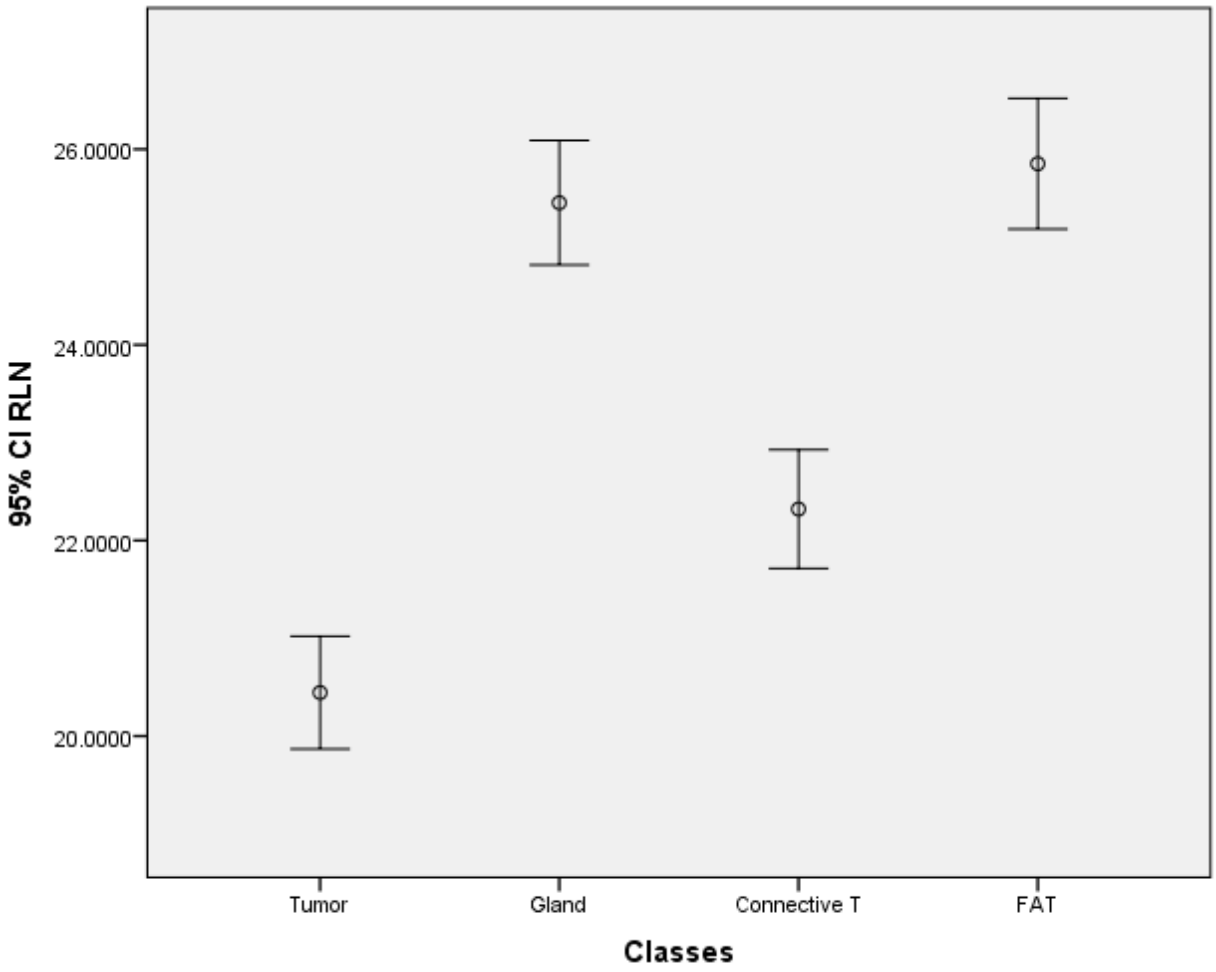

Fig .4.8 show error bar plot for the CI RLN textural features that selected by the linear stepwise discriminate function as a discriminate between all features. From the discriminate power point of view in respect to the applied features the RLN can differentiate between all the classes successfully.

`

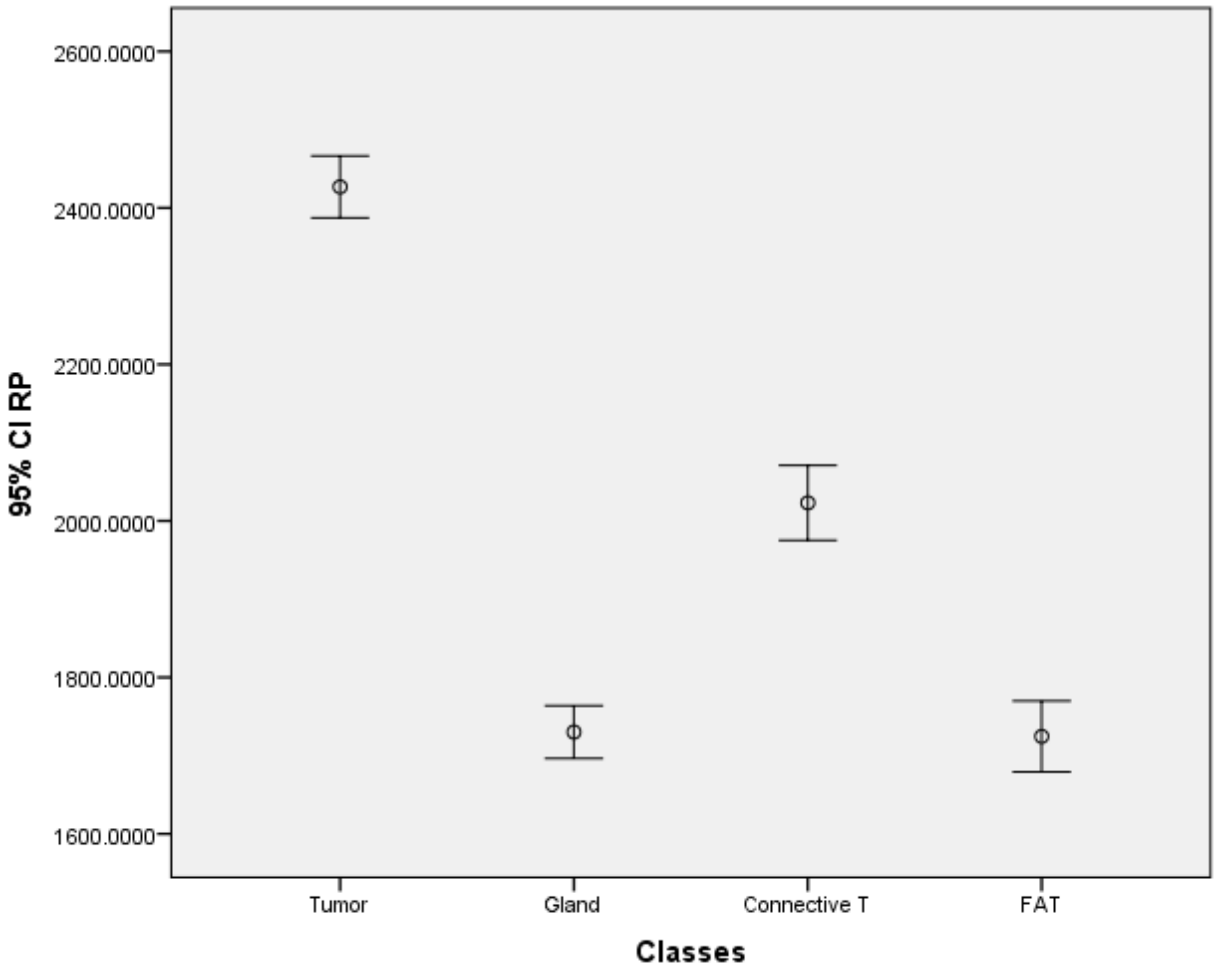

Fig 4.9. show error bar plot for the CI RP textural features that selected by the linear stepwise discriminate function as a discriminate feature where it discriminates between all features.

`

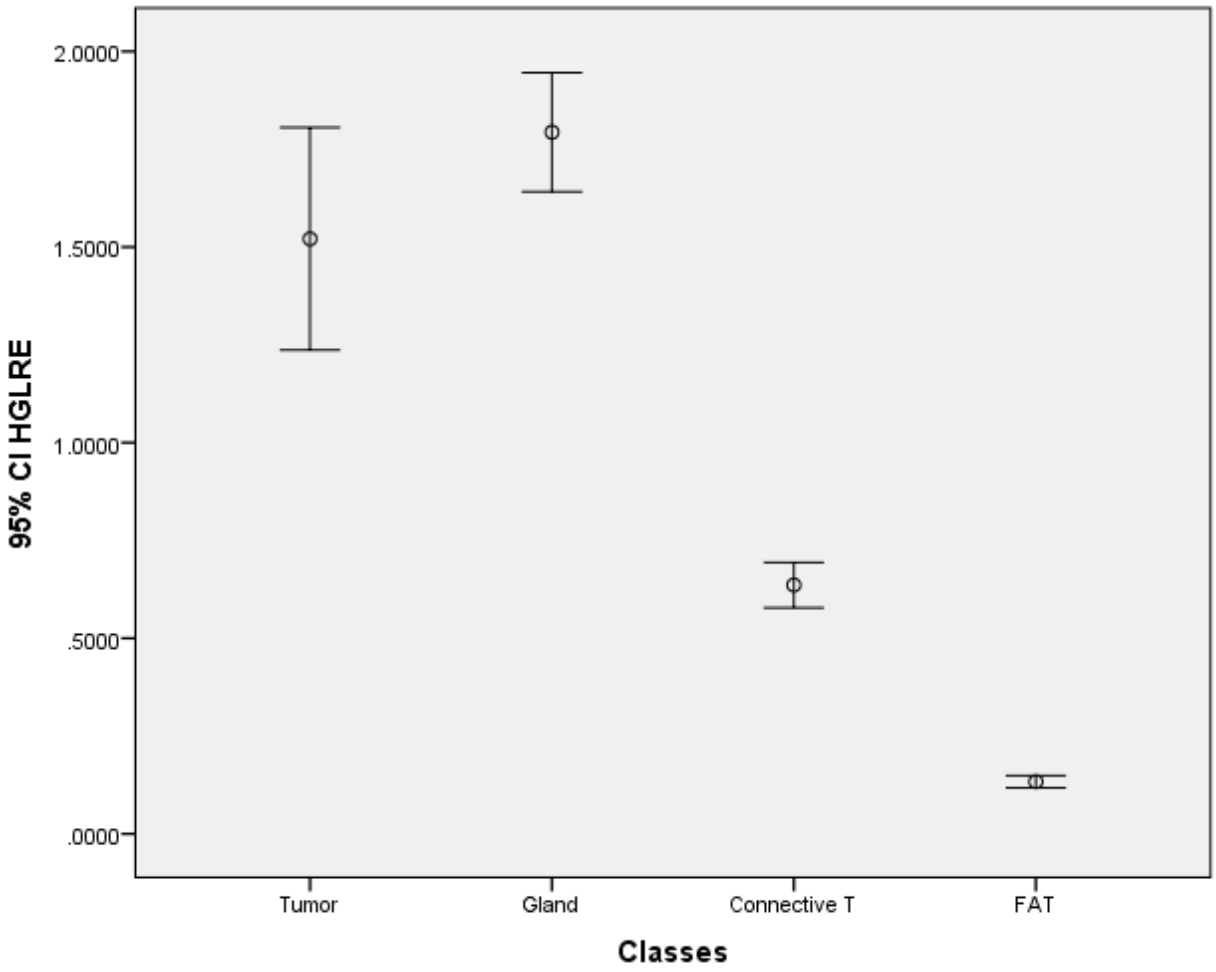

Fig 4.10. show error bar plot for the CI HGLRE textural features that selected by the linear stepwise discriminate function as a discriminate between all features. From the discriminate power point of view in respect to the applied features the HGLRE can differentiate between all the classes successfully.

`

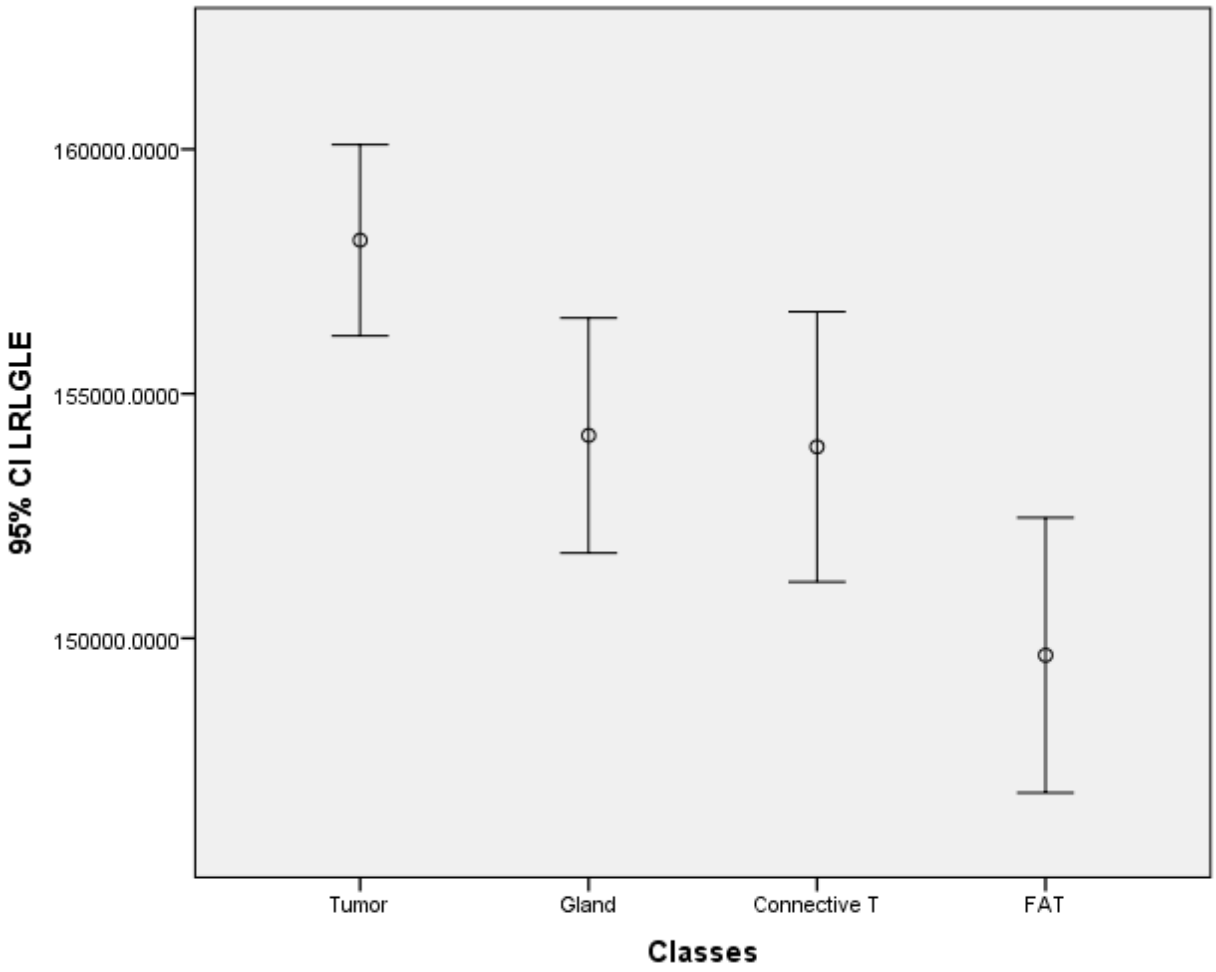

Fig 4.11. show error bar plot for the CI LRLGLE textural features that selected by the linear stepwise discriminate function as a discriminate feature where it discriminates between all features.

`

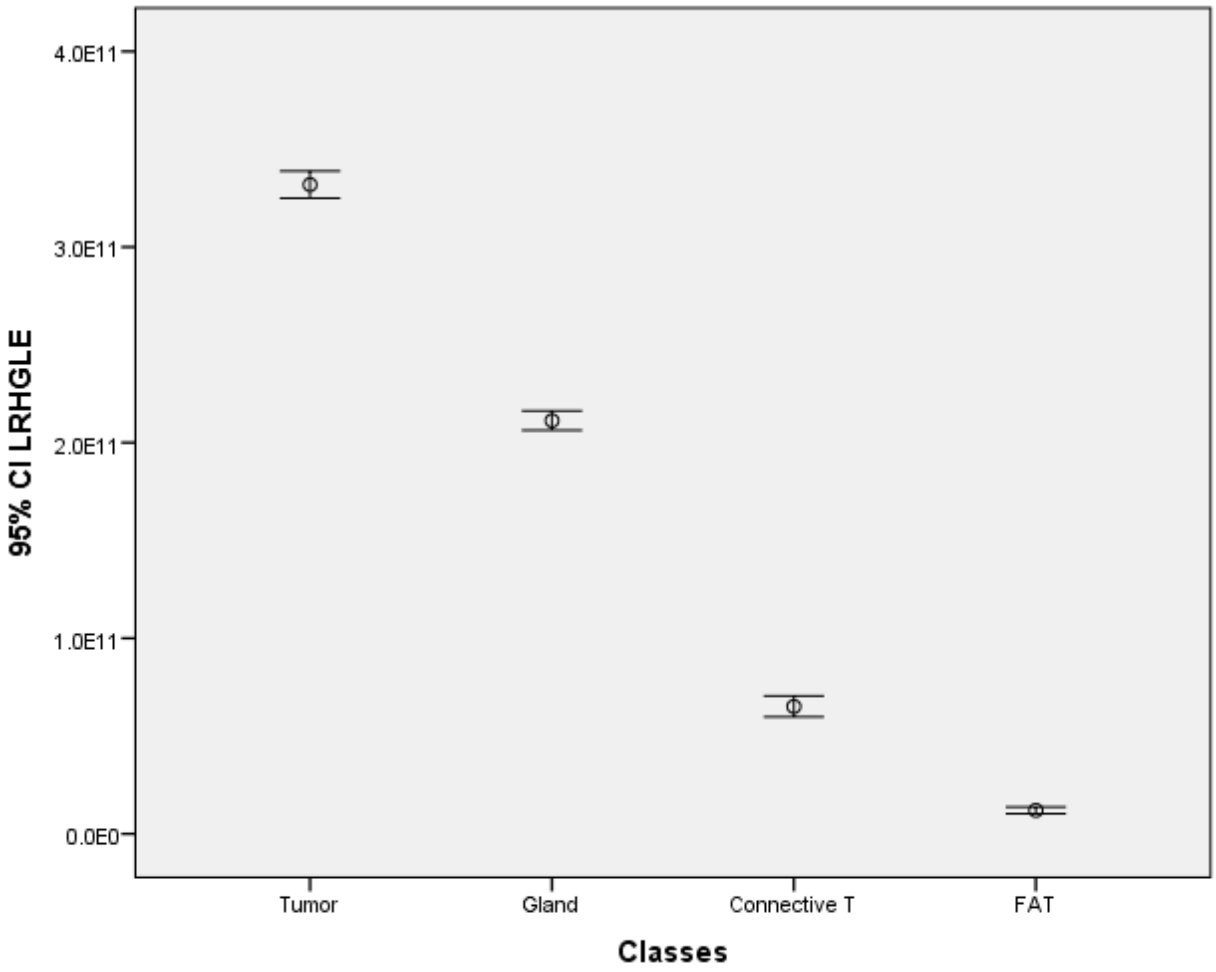

Fig 4.12. show error bar plot for the CI LRHGLE textural features that selected by the linear stepwise discriminate function as a discriminate between all features. From the discriminate power point of view in respect to the applied features the LRHGLE can differentiate between all the classes successfully.

4.3 Original mammogram image and the image processed by IDL:

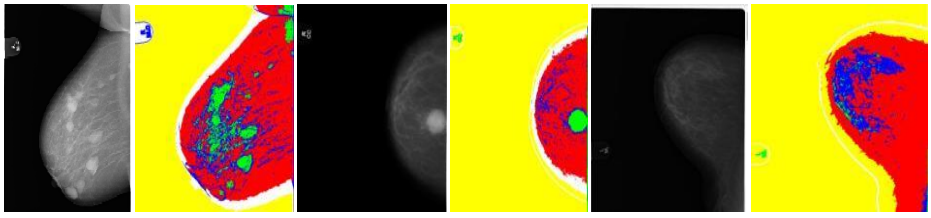

Malignat Benign Normal

Fig4.13 Mammogram image versus processed by IDL

`

Chapter Five

Discussion, Conclusion and Recommendation

5.1Discussion:

This study was made to characterize the breast mass by comparing to normal breast tissue (fat, connective and glandular) in digital mammogram by using IDL programming language as platform to generate codes.

The sample was taken randomly from X-ray department at cancer medical diagnostic center. There are 155 digital mammogram images in normal and abnormal categories which are transformed by using the IDL processing program firstly by using first order statistics which are (Mean, Stander Deviation and Energy) and the data discriminated by using SW-LDA in SPSS the result was for

Feature extraction by using first order statistics:

Table4.1 show classification score matrix generated by linear discriminate analysis and the overall classification accuracy of breast masses and breast tissue 94.0%, were the classification accuracy of gland 86.8%, fat 98.2%, connective tissue 98.9%, While the tumor showed a classification accuracy 98.5%.

94.0% of original grouped cases correctly classified

Fig 4.1 scatter plot demonstrates the distribution of four Classes according to their textural feature using linear discriminate analysis functionsthe classification showed that the breast tissues was classified well from the rest of the tissues although it has characteristics mostly similar to surrounding tissue.

Fig .4.2 show error bar plot for the CI mean textural features that selected by the linear stepwise discriminate function as a discriminate between all features. From

`

the discriminate power point of view in respect to the applied features the mean can differentiate between all the classes successfully.

Fig 4.3.show error bar plot for the CI energy textural features that selected by the linear stepwise discriminate function as a discriminate feature where it discriminates between all features.

Fig 4.4 show error bar plot for the CI standard deviation textural features that selected by the linear stepwise discriminate function to discriminates between all features. From the discriminate power point of view in respect to the applied features the STD can differentiate between all the classes successfully.

Feature extraction by using higher order statistics:

Feature extracted from 155 mammogram images by using a set of 6 Grey-level run-length matrix**(** GLRLM)features (long run emphasis (LRE) , grey level non uniformity (GLN), run length non uniformity (RLN), Run percentage (RP), High Gray Level Run Emphasis (HGLRE) and Low Gray Level Run Emphasis (LRHGLE), discriminated analysis used and the result was:

Table 4.2. show classification score matrix generated by linear discriminate analysis and the overall classification accuracy of breast masses 91.5%, were the classification accuracy of gland 98.9%, fat 86.3%, connective tissue 91.9%, While the tumor showed a classification accuracy 88.9%.

91.5% of original grouped cases correctly classified

`

Fig 4.5. scatter plot demonstrates the distribution of four Classes according to their textural feature using linear discriminate analysis functions

the classification showed that the breast tissues was classified well from the rest of the tissues although it has characteristics mostly similar to surrounding tissue.

Fig .4.6. show error bar plot for the CI LRE textural features that selected by the linear stepwise discriminate function as a discriminate between all features. From the discriminate power point of view in respect to the applied features the LRE can differentiate between all the classes successfully.

Fig 4.7. show error bar plot for the CI GLN textural features that selected by the linear stepwise discriminate function as a discriminate feature where it discriminates between all features.

Fig .4.8 show error bar plot for the CI RLN textural features that selected by the linear stepwise discriminate function as a discriminate between all features. From the discriminate power point of view in respect to the applied features the RLN can differentiate between all the classes successfully.

Fig 4.9. show error bar plot for the CI RP textural features that selected by the linear stepwise discriminate function as a discriminate feature where it discriminates between all features.

Fig 4.10. show error bar plot for the CI HGLRE textural features that selected by the linear stepwise discriminate function as a discriminate between all features. From the discriminate power point of view in respect to the applied features the HGLRE can differentiate between all the classes successfully.

Fig 4.11. show error bar plot for the CI LRLGLE textural features that selected by the linear stepwise discriminate function as a discriminate feature where it discriminates between all features.

`

Fig 4.12. show error bar plot for the CI LRHGLE textural features that selected by the linear stepwise discriminate function as a discriminate between all features. From the discriminate power point of view in respect to the applied features the LRHGLE can differentiate between all the classes successfully.

`

5.2 Conclusion:

Digital imaging technology have become indispensable components for clinical procedures. This study highlight on evaluation of mass extra marginal detection using image processing programs (IDL), once we need faster and accurate diagnostic modalities in this situation in order to have high diagnostic accuracy in assessing breast tumors and therefore using this scans to plan patient for treatment which need Avery accurate delineation of tumor edges in case of CTV and planning target volume in order to deliver sufficient dose in case of radiation to the both volumes and increase therapeutic and diagnostic radio.

The texture reveals a different pattern of the mass and the other normal breast tissue (fat, glandular and connective tissues) by using first order statistics with classification accuracy of 94% and when we used higher order statistics the classification accuracy was 91.5% so we found that mammographic texture analysis is a reliable technique for differential diagnosis of breast tumors and breast tissue. Furthermore, the combination of imaging-based diagnosis and texture analysis can significantly improve diagnostic performance.

`

5.3. Recommendation:

- Texture analysis can be integrated in mammography as Computer Aided Diagnosis method to reduce the operator dependent concept in mammography field and hence reduce using of unnecessary fine meddle aspiration.
- Young patient with positive family history must be followed and screened routinely by ultrasound and texture analysis to detect small dense lesion that can be missed by mammogram.
- Texture analysis tools are not usually available, and it is expensive. According to its high values in diagnosis of breast lesion and differentiation between it is types, study advised that to indorse it, until becomes available to any radiology department and patient.
- Further studies should be carried out in this field on many aspects such as increasing the number of patients, to show the relation between benign and malignant breast tumors.
- Also Further studies should be carried, diagnosis of breast morphological result and consideration of scanning time to be equal in all patients.
- Compare between the role of mammography scanning and other diagnostic tools using .

`

References:

Abraham Chandy, D., Stanly Johnson, J.,& Easter Selvan, S. (2014). “Texture feature extraction using gray level statistical matrix for content-based mammogram retrieval”, Multimed Tools Appl.vol 72, 2,2011-2024.

A Guide to Mammography and Other Breast Imaging Procedures Recommendations of the NATIONAL COUNCIL ON RADIATION PROTECTION AND MEASUREMENTS Issued December 31, 2004.(NCRP report No.149).

Akay, M. (2006). Wiley of Encyclopedia of Biomedical Engineering (1st edition). John Wiley & Sons.

Answers.com. "Oncology Encyclopedia: Cystosarcoma Phyllodes". Archivedfrom the original on 8 September 2010. Retrieved 10 August 2010.

Aswini kumar Mohanty, Manas Ranjan Senapati, Swapnasikta Beberta, Saroj Kumar Lenka Texturebased features for classification of mammograms using decision tree . Neural Comput & Applic(2013) 23:10111017.

Bronzino, Joseph D., 1937- 2000. The biomedical engineering handbook

Cardenosa, Gilda (2004). Breast Imaging. Lippincott Williams & Wilkins.

Bluekens, A. M. J., Karssemeijer, N., Beijerinck, D., Deurenberg, J. J. M., van Engen, R. E., Broeders, M. J. M., & den Heeten, G. J. (2010). Consequences of

`

digital mammography in population-based breast cancer screening: initial changes and long-term impact on referral rates. European radiology, 20(9), 2067-73.

Elfadel, I.M. and R.W. Picard, Gibbs Random Fields, Cooccurrences, and Texture Modeling. IEEE PAMI (A longer version is appeared in: Technical Report #204,M.I.T, Media Lab, Perceptual Computing, 1993), 1994. 16(1): p. 24-37

Bruce, V.; Georgeson, M. & Green, P. (2003). Visual Perception: Psychology and Ecology.Psychology Press Publications, ISBN 1841692387, UK.

Basset LW, Kimme-Smith C (1991) Breast sonography. AJR 156:449–455

Campbell S, Bhan V, Royston P, Whitehead MI, Collins WP (1990a) .

Cardenosa, Gilda (2004). Breast Imaging. Lippincott Williams & Wilkins.

Chianyama Catherine N. (2004). Breast Diseases: Radiology, Pathology, Risk Assessment. SpringerVerlag Berlin Heidelberg New Yorkublishing, Ed.

Chu A, Sehgal CM (1990) Use of gray value distribution of run lengths for texture analysis. Pattern Recognit Lett 415–420.

Consequences of digital mammography in population-based breast cancer screening: initial changes and long-term impact on referral rates. European radiology, 20(9), 2067-73.

Dasarathy BV, Holder EB (1991) Image characterizations based on joint gray level—run length distributions. Pattern Recognit Lett 12(8):497–502.

`

Dixon JM, Ravisekar O, Chetty U et al. Periductal mastitis and duct ectasia: different conditions with different a etiologies. BrJSurg 1996;83:820–822.

Dixon, J. M. (2006). ABC of breast diseases. (3rd ed.) B. Publishing, Ed.

EMedicine (23 August 2006). "Breast Cancer Evaluation". Archived from the original on 12 February 2008. Retrieved 5 February 2008.

Engeland, S. V., Snoeren, P., Hendriks, J., & Karssemeijer, N. (2003). Mammogram Registration, 22(11), 1436-1444.

F Tomita and S Tuji, Computer analysis of visual texture, Kluwer, Norwel, M.A 1990.

Guyton, A. C., & Hall, J. E. (2000). Textbook of Medical Physiology (10th ed.). (W. S. Company, Ed.).

Haralick , RM., Shanmugam, K., &Dinstein, I.(1973).“Textural features for image classification”,IEEE Trans Syst Man Cybern ,vol 3,issue:6, 610–621.

Haralick, R.M., Watson, L.: A facet model for image data. Comput. Vision Graphics Image Process 15, 113–129, 1981.

Hashimoto, Beverly (2008). Practical Digital Mammography. Thieme Medical Publishers..

Jain, A.K. &Chandrasekaran. (1982). Dimensionality and sample size considerations. In:Pattern Recognition in Practice, Krishnaiah, P.R. &Kanal, L.N., Vol. 2, pp. 835-888.North Holland.

`

Jain, A.K. &Zongker, D. (1997). Feature selection: evaluation, application and small sample performance. IEEE Transactions on Pattern Analysis and Machine Intelligence, Vol. 2, No. 19, pp. 153-158.

Jatoi, I., & Kaufmann, M. (2010). Management of breast diseases. Springer, Ed..

Alvin, Siverstein, V., & Nunn, L. S. (2006). Cancer. (L. of congress cataloging in Publication, Ed.)

Johnson KC, Miller AB, Collishaw NE, Palmer JR, Hammond SK, Salmon AG, Cantor KP, Miller MD, Boyd NF, Millar J, Turcotte F (Jan 2011).

Julesz, B. (1975). Experiments in the visual perception of texture. Scientific American, Vol. 232, pp 34-43.

Kopans, Daniel B. (2007). Breast Imaging (3rd edition). Lippincott Williams & Wilkins.

Lacroix M (December 2006). "Significance, detection and markers of disseminated breast cancer cells". Endocrine-Related Cancer. **13** (4): 1033–67. doi:10.1677/ERC-06-0001. PMID 17158753.

Malik, M. A. N. (2010). Breast Diseases ; 17(3), 366-372.

Manavalan Radhakrishnan and Thangavel Kuttiannan Comparative Analysis of Feature Extraction Methods for the Classification of Prostate Cancer from TRUS Medical Images. IJCSI International Journal of Computer Science Issues, Vol. 9, Issue 1, No 2, January 2012, ISSN (Online): 1694-0814.

`

Merck Manual of Diagnosis and Therapy (February 2003). "Breast Disorders: Overview of Breast Disorders". Archived from the original on 3 October 2011. Retrieved 5 February 2008.

Moinfar, F. (2007). Essentials of diagnostic breast pathology. Springer. Moore, K. L., Agur, A. M., & Dalley, A. F. (2004). Essential Clinical Anatomy. (4nd ed.). (W. Kluwer, Ed.)

Moorman C, Pennypacker H, Pierce P, Sciandra E, Smith R, Coates R (2004).

National Cancer Institute (27 June 2005). "Paget's Disease of the Nipple: Questions and Answers". Archived from the original on 10 April 2008. Retrieved 6 February 2008.

National Cancer Institute (1 September 2004). "Metastatic Cancer: Questions and Answers". Archived from the original on 27 August 2008. Retrieved 6 February2008.

Nees, A. V. (2008). Digital mammography: are there advantages in screening for breast cancer? Academic radiology, 15(4), 401-7.

Panno, J. (2005). Cancer: the role of genes, lifestyle and environment. Library of congress cataloging in Publication.

Perez, Reinaldo J. (2002). Design of medical electronic devices. Academic Press.

Pietikainen, M.K. (ed) (2000). Texture analysis in machine vision, World Scientific Publishing, 981-02-4373-1, Singapore.

`

Pisano, Etta D.,Yaffe, Martin J., Kuzmiak, & Cherie M.(2004). Digital Mammography. Lippincott Williams & Wilkins.

Qin, X. and Y.H. Yang, Basic Gray Level Aura Matrices: Theory and its Application to Texture Synthesis. IEEE ICCV, Beijing, China, 2005: p. 128-135.

Saslow D, Hannan J, Osuch J, Alciati MH, Baines C, Barton M, Bobo JK, Coleman C, Dolan M, Gaumer G, Kopans D, Kutner S, Lane DS, Lawson H, Meissner H,).

Saunders, Christobel; Jassal, Sunil (2009). Breast cancer (1. ed.). Oxford: Oxford University Press. p. Chapter 13. ISBN 978-0-19-955869-8. Archived from the original on 25 October 2015.

Seeley, R., Stephens, T., & Tate, P. (2004). Anatomy and Physiology. The McGraw−Hill Company.

Sivaramakrishna, R., & Gordon, R. (1997) Detection of Breast Cancer at a Smaller Size Can Reduce the Likelihood of Metastatic Spread: A Quantitative Analysis.

Tartar, Marie, Comstock, Christopher E., Kipper, & Michael S. (2008). Breast Cancer Imaging:A Multidisciplinary, Multimodal Approach. Mosby Elsevier.

Tang X (1998) Texture information in run-length matrices. IEEE Trans Image Process 7(11):1602–1609.

Watson M (2008). "Assessment of suspected cancer". InnoAiT. **1** (2): 94–107. doi:10.1093/innovait/inn001.

Acad Radiol, Association of University Radiologists, Canadá, v. 4, n. 1, p. 8-12.

`

Webster, J. (2006). Encyclopledia of Medical Devices and Instrumentation (2nd ed., Vol. 4). U.S.: Wiley Insterscience.

Zhang, J., Li, G-l.,& He, S-w. (2008). “Texture-based image retrieval by edge detection matching GLCM”. Proceedings of the 10 international conference on high performance computing and communications

Zohra Haliche,& Kamal Hammouche. (2011) “The gray level aura matrices for textured image segmentation”,Analog Integr Circ Sig Process, vol. 69, 29-38.